January 2016

Modeling of Bread Structure Based on Mixed Cell Foams

Heather M. Lavoie
Worcester Polytechnic Institute

Rachel A. Komara
Worcester Polytechnic Institute

WPI

MODELING OF BREAD STRUCTURE BASED ON MIXED CELL FOAMS

A Major Qualifying Project Proposal
submitted to the Faculty of
WORCESTER POLYTECHNIC INSTITUTE
in partial fulfillment of the requirements for
the Degree of Bachelor of Science

Submitted by:

_____
Rachel A. Komara

_____
Heather M. Lavoie

January 14, 2016

Approved by:

_____
Professor Satya Shivkumar, Advisor

Department of Mechanical Engineering

ABSTRACT

The texture of bread is strongly influenced by the cell structure and the extent of staling during storage. The goal of this project was to examine and analyze the effect of stress on cell structure. Bread crumb was digitally modeled in both MATLAB and SolidWorks, tensile testing was performed with an Instron machine, and microscopes were used to visually inspect the effects of force and the fracture pattern. The results indicated that the open and closed cell ratio of bread crumb does not initially change within the testing period of one week. The cells elongate in the direction of the tensile force and the cell wall ruptures at high stresses, with a mixed intracellular and transcellular fracture. Staling does not have a significant effect on cell structure.

ACKNOWLEDGEMENTS

The authors of this report would like to thank the Mechanical Engineering Department at Worcester Polytechnic Institute for assistance on this project. More specifically, Satya Shivkumar, Mechanical Engineering Professor, for his continued guidance throughout the entirety of this project; Siamak Ghorbani Faal, PhD Candidate, for his instruction on the creation of digital models; and Rita Shilansky, Administrative Assistant, for her help obtaining supplies and access to the Instron machine. Without their help and support, this project's accomplishments would not have been possible.

TABLE OF CONTENTS

Abstract 1
Acknowledgements 2
Table of Contents 3
List of Figures 5
List of Tables 7
Chapter 1: Introduction 8
Chapter 2: Literature Review 10
2.1 Structure of Bread 10
2.2 Cellular Formed Solids 12
2.3 Properties of Bread 14
2.3.1 Mechanical Properties 15
2.4 Theoretical Modeling 16
2.4.1 Honeycomb Structure 16
2.4.2 Digital Model for Bread Crumb 19
2.4.2.1 Development of Digital Model 19
2.4.2.2 Application of Digital Model 20
Chapter 3: Objectives 21
Chapter 4: Methodology 22
4.1 SolidWorks Model 22
4.2 MATLAB Code 25
4.2.1 Random Distribution of Cells 30
4.2.2 Volume and Density 31
4.2.3 Open and Closed Cell Ratio 31
4.3 Tensile Testing Bread 32
4.3.1 Initial Trials 33
4.3.2 Standardized Procedure 35
Chapter 5: Results and Discussion 37
5.1 MATLAB Modeling 37
5.2 Analytical Analysis 40
5.2.1 Mechanical Properties 42

5.2.2 Comparison to Literature 48
5.3 Comparison of Graphical Plots 50
5.4 Comparison of Microscopic Images 56
Chapter 6: Conclusions 60
References 61
Appendix A: Day 1 MagniSci Data 63
Appendix B: Day 3 MagniSci Data 64
Appendix C: Day 5 MagniSci Data 65
Appendix D: Day 7 MagniSci Data 66
Appendix E: MATLAB Code: BreadGen 67
Appendix F: MATLAB Code: CollisionDetection_II 70
Appendix G: MATLAB Code: CloseCollision 71
Appendix H: MATLAB Code: Box2Data 72
Appendix I: MATLAB Code: Hex2Data 73
Appendix J: MATLAB Code: Points2Mesh 74
Appendix K: MATLAB Code: PlotMesh 75
Appendix L: MATLAB Code: Convert2STL 76

LIST OF FIGURES

Figure 1: Hierarchal structure of bread crumb (Liu & Scanlon, 2003). 10
Figure 2: Progression of cellular expansion and coalescence (Scanlon & Zghal, 2001). 11
Figure 3: Central portion of bread crumb (Scanlon & Zghal, 2001). 12
Figure 4: Open and closed cell structures (Gibson & Ashby, 1999). 13
Figure 5: Mechanical stress and strain of tensile testing foams (Gibson & Ashby, 1999). 14
Figure 6: Typical stress and strain behavior of bread crumb under loads 15
Figure 7: Various shapes for cellular solids (Gibson & Ashby, 1999). 17
Figure 8: SolidWorks model with randomly located and sized cylindrical structures 23
Figure 9: Hexagonal structures with both open and closed cells. 24
Figure 10: Resulting forces on the hexagonal structure from a 1N tensile load. 24
Figure 11: Initial model of an entire loaf of bread with rectangular open cells. 25
Figure 12: Closer look at the cellular structures inside of the bread model. 26
Figure 13: Single slice of bread with rhombic dodecahedral cellular bodies inside. 27
Figure 14: View from the front plane of the cellular structures inside of the bread body. 28
Figure 15: SolidWorks figure created from the MATLAB plots shown in Figures 13 and 14. ... 29
Figure 16: Closer view of the open cells in the SolidWorks solid body. 29
Figure 17: Delaunay Triangulation. This illustrates the result of the function 30
Figure 18: Instron Model 4201 used for tensile testing. 32
Figure 19: Example of a bread sample for tensile testing. Note the dimensions. 33
Figure 20: Comparison of the video camera and camera footage 34
Figure 21: Post-fracture samples prepared for microscopic analysis. 35
Figure 22: Final setup for tensile testing of bread samples and recording the tensile data. 36
Figure 23: MATLAB model with the dimensions of one tensile test specimen. 37
Figure 24: Initial open-cells compared to the final number of cells 38
Figure 25: Initial number of open-cells. 39
Figure 26: Total cellular bodies present in the samples. 39
Figure 27: Hexagonal prisms and rhombic dodecahedral prisms 42
Figure 28: Illustration of hexagonal prisms and rhombic dodecahedral prisms 42
Figure 29: Mechanical properties of tensile tested bread crumb by daily comparison. 45
Figure 30: Tensile properties by increasing open-closed cell ratio, from left to right. 46

Figure 31: Average stress vs. strain by day for tensile samples. 47
Figure 32: The elastic open-cell force vs. time, as calculated with the given constant k=1. 49
Figure 33: The elastic open-cell force vs. time 49
Figure 34: Comparison of the effect of elastic modulus during linear behavior. 50
Figure 35: Day 1 Sample 10 force vs. time graph 51
Figure 36: Time lapse of Day 1 Sample 10 photos during fracture 51
Figure 37: Day 3 Sample 7 force vs. time graph 52
Figure 38: Time lapse of Day 3 Sample 7 photos during fracture 53
Figure 39: Day 7 Sample 11 force vs. time graph 54
Figure 40: Time lapse of Day 7 Sample 11 photos during fracture 54
Figure 41: Pre- and post-fracture microscopic analysis of bread crumb. 56
Figure 42: Post-fracture analysis of the break in cell wall structure. 57
Figure 43: MagniSci analysis report of cell fraction 58
Figure 44: Fracture zone of bread crumb, note the angled break. 58

LIST OF TABLES

Table 1: Relative density equations by shape of cellular solid (Gibson & Ashby, 1999). 18
Table 2: MATLAB generated values of the finalized model. 38
Table 3: MagniSci data of experimental samples. 40
Table 4: MagniSci data summarized by daily averages. 41
Table 5: Calculation of constants for cellular structures. 44
Table 6: Sample strength and modulus values by day. 47
Table 7: Comparison of constants, given versus experimental. 48
Table 8: Growth rate of presented samples. 55
Table 9: Complete MagniSci data for the three best samples on Day 1. 63
Table 10: Complete MagniSci data for the three best samples on Day 3. 64
Table 11: Complete MagniSci data for the three best samples on Day 5. 65
Table 12: Complete MagniSci data for the three best samples on Day 7. 66

CHAPTER 1: INTRODUCTION

Bread, a basic staple of the human diet, has been around for thousands of years. Throughout the world, bread is composed of a variety of ingredients, which each serve different purposes in the establishment of texture and flavor. The most basic ingredients include water, flour, a form of leavening agent such as yeast or other chemicals, and sodium chloride (Scanlon & Zghal, 2001). The procedures taken to mix the ingredients before baking can directly affect the resulting crumb structure. In general, three main steps are involved in processing the dough in order to create a loaf with mechanical properties that promote gas retention, which yields a well-expanded loaf of bread. These key processing steps include mixing and developing the dough through fermentation, creating a foam-like structure in the dough through shaping and proofing, and allowing the dough to undergo changes in molecular configuration through baking (Scanlon & Zghal, 2001).

The difference in crumb structure between freshly baked breads and commercial breads is mainly a result of additives, also known as bread improvers, which can shorten the time required for rising and lengthen the shelf-life (Stampfli & Nersten, 1995). Emulsifiers are also known to provide a crumb structure that is finer and more uniform in grain and cell size. These properties are important for mass-produced bread, which must withstand transportation conditions and varying days of shelf-life. The bread used throughout this project was store-brand, pre-packaged white bread.

The goals of this project were to create a digital model of bread crumb yielding a porosity and density comparable to that of physical bread, to then 3D print the resulting model, and finally perform tests on the printed model in order to determine its mechanical properties. Several approaches were taken in attempt to achieve these initial goals. The project then progressed into a

focus on tensile testing the bread and analyzing how the cells change as a function of time, force, and elongation.

In Chapter 2, background information regarding bread properties and crumb structure is presented. Goals and objectives are described in Chapter 3, while the procedures followed in order to achieve them are explained in Chapter 4. The methodology is followed by a discussion of the resulting data and findings in Chapter 5, as well as conclusions and recommendations in Chapter 6.

CHAPTER 2: LITERATURE REVIEW

2.1 STRUCTURE OF BREAD

Bread crumb is generally seen as a two-phase soft cellular solid, consisting of a solid phase apparent in the cell wall structure and a fluid phase made up of air. These two phases can be seen when observing the cross-sectional area of bread crumb (Scanlon & Zghal, 2001). In the two dimensional cross-sectional view, it is clear that the bread crumb is one connected entity. The physical makeup of bread crumb from a food engineering perspective can be seen in the following Figure 1.

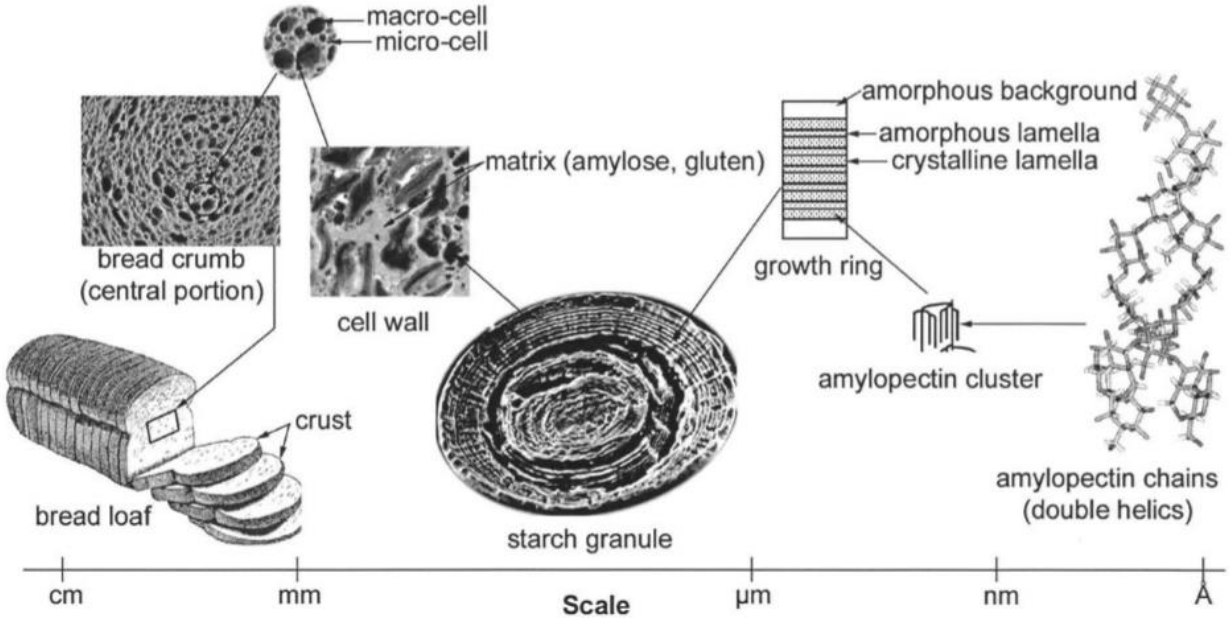

Figure 1: Hierarchal structure of bread crumb (Liu & Scanlon, 2003).
This figure illustrates the structure of bread crumb, from the basic loaf down to its amylopectin chains.

According to microscopic evidence, when observed in three dimensions, the bread crumb is not necessarily entirely connected, but it is mostly connected (Scanlon & Zghal, 2001). The ratio of the two present phases and the extent of their connectivity has an effect on structure, and therefore the bread crumb's properties.

The structure of bread is formed by a series of physical processes, yielding a wide variety in properties among different areas of the bread crumb. Figure 2 below illustrates the growing cells when undergoing the baking process.

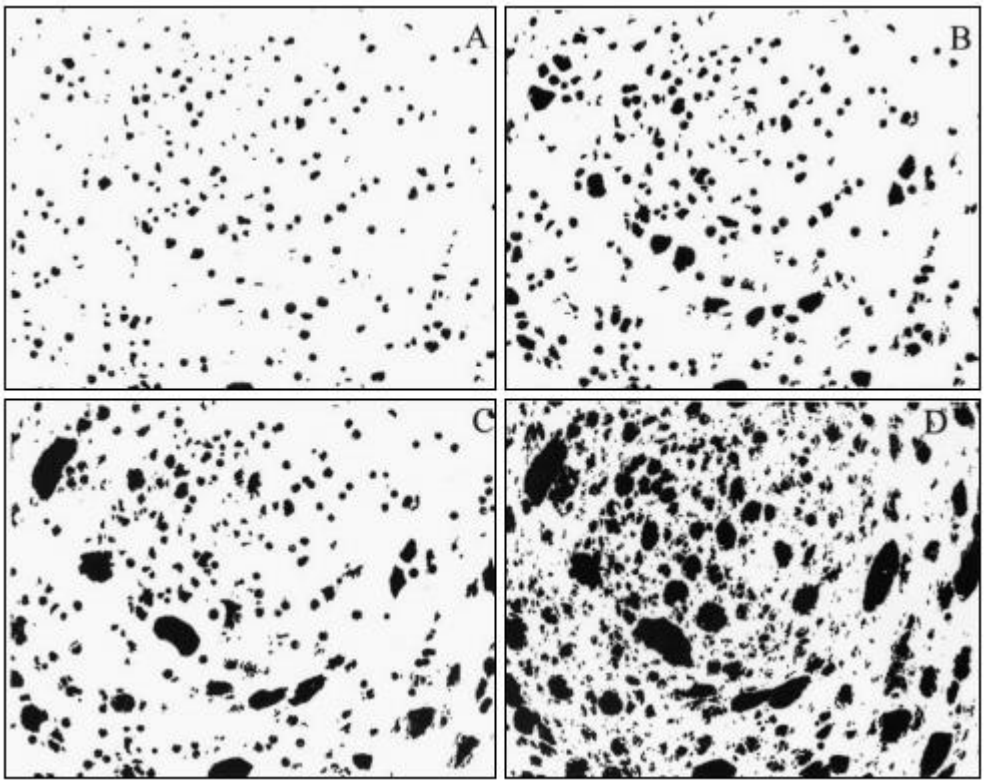

Figure 2: Progression of cellular expansion and coalescence in gas cells of bread crumb (Scanlon & Zghal, 2001). This figure illustrates the growth of cells as they expand and fracture cell walls.

Expansion within the dough while baking causes coalescence and fracture in these gas cells (Wang, Austin, & Bell, It's A Maze: The Pore Structure of Bread Crumbs , 2011). Varying location and properties of cell walls, as well as potential imperfections in the general cellular structure, all have an effect on mechanical properties and behavior (Zghal, Scanlon, & Sapirstein, 2002). Figure 3 below provides sufficient magnification to see the open cell shapes as well as provide an idea of cell wall thicknesses relative to the open cells.

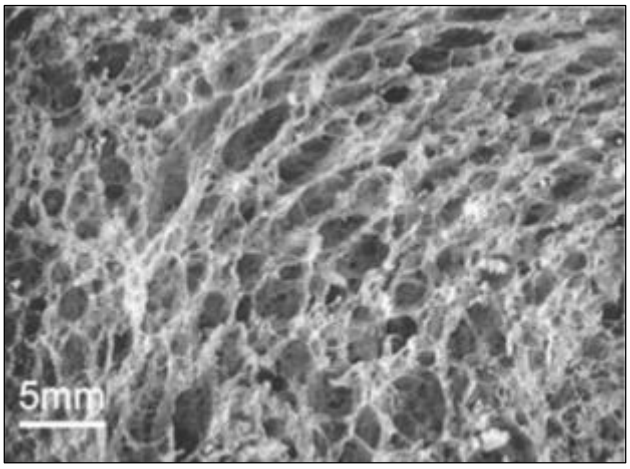

Figure 3: Central portion of bread crumb (Scanlon & Zghal, 2001).
This figure illustrates the variety in cellular shape and size of the crumb, scale provided.

Density and crumb features, such as cell areas and wall thicknesses, are useful structural properties in analyzing bread crumb. Furthermore, macroscopic inspection of bread slices yielded cell diameters with values between 1.23 mm and 2.00 mm in the crumb (Wang, Austin, & Bell, It's A Maze: The Pore Structure of Bread Crumbs , 2011).

2.2 CELLULAR FORMED SOLIDS

A cellular formed solid is defined as "one made up of an interconnected network of solid struts or plates which form the edges and faces of cells" (Gibson & Ashby, 1999). The simplest two-dimensional structure is the honeycomb, which can pack together efficiently in three dimensions. The solid material in the overall structure is one body consisting of closed cells and making up the edges of opened cells. Bread, when investigated as a natural foam structure, shows a wide variety in cellular structure and is generally comprised of a mixture of open and closed cells. In Figure 4 below, a foam made of open cells is shown on the left, and a foam made of closed cells is illustrated on the right.

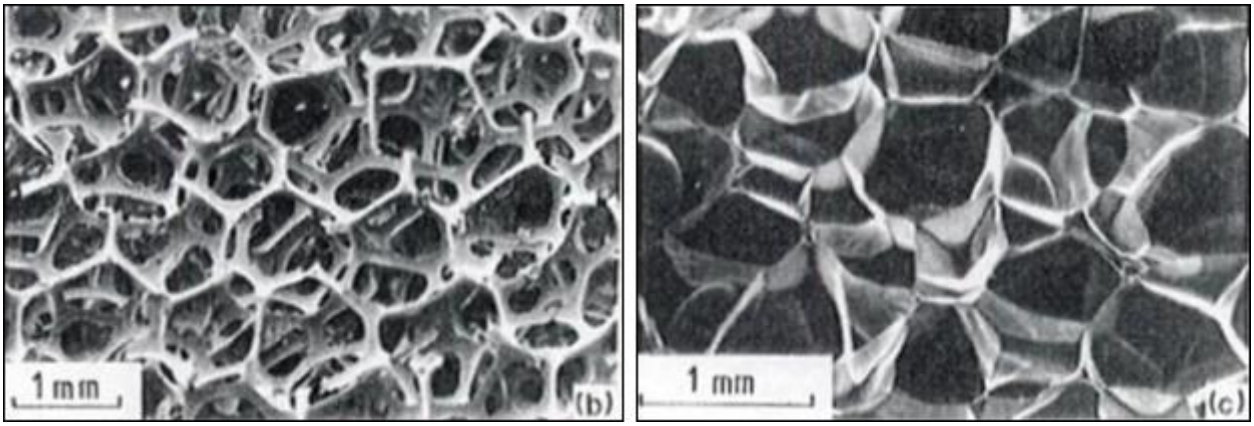

Figure 4: Open and closed cell structures (Gibson & Ashby, 1999).
On the left, an open-celled structure is shown, while on the right, a structure with closed cells is depicted.

The cellular formation of bread crumb has an effect on texture of the bread crumb, and as a force is applied to the crumb, its texture is affected as a result. Texture and structure are inherently linked in the mechanics of bread crumb. Cellular properties most attributed to the texture of bread crumb are the cellular size, uniformity, and wall thickness (Scanlon & Zghal, 2001). Bread crumb with a uniform distribution of smaller, finely shaped cells with thin walls yields a softer texture as opposed to crumb with a variety of cell sizes and wall thicknesses (Scanlon & Zghal, 2001).

Another factor which must be considered in the texture and structural properties of bread is staling. As bread stales, starch molecules inside the crumb crystallize and result in a harder texture that feels as if it has dried out. This is not the case, as the crystallization process requires both free water molecules and air. Literature has hypothesized that this crystallization and change in the intra-granular amylose fraction has an effect on the texture and mechanical properties of bread crumb, creating the feeling of rigidity (Hug-Iten, Handschin, Conde, & Escher, 1999). In theory, fracture of a foam structure with greater rigidity would result in brittle fracture with little elasticity.

2.3 PROPERTIES OF BREAD

Bread properties and crumb structure are crucial in determining visual crumb appearance such as color and physical texture, and bread quality such as taste. When visually examining the crumb appearance, numerous methods of image acquisition can be used, some of which include transmission of light, reflection of light, and addition of reagents (Scanlon & Zghal, 2001). Moreover, the mechanical behavior of the bread crumb alone is very intricate. This behavior is characterized by mechanical testing including tension, compression, and shear. The mechanical stress and strain curves of tension can be seen in the following Figure 5.

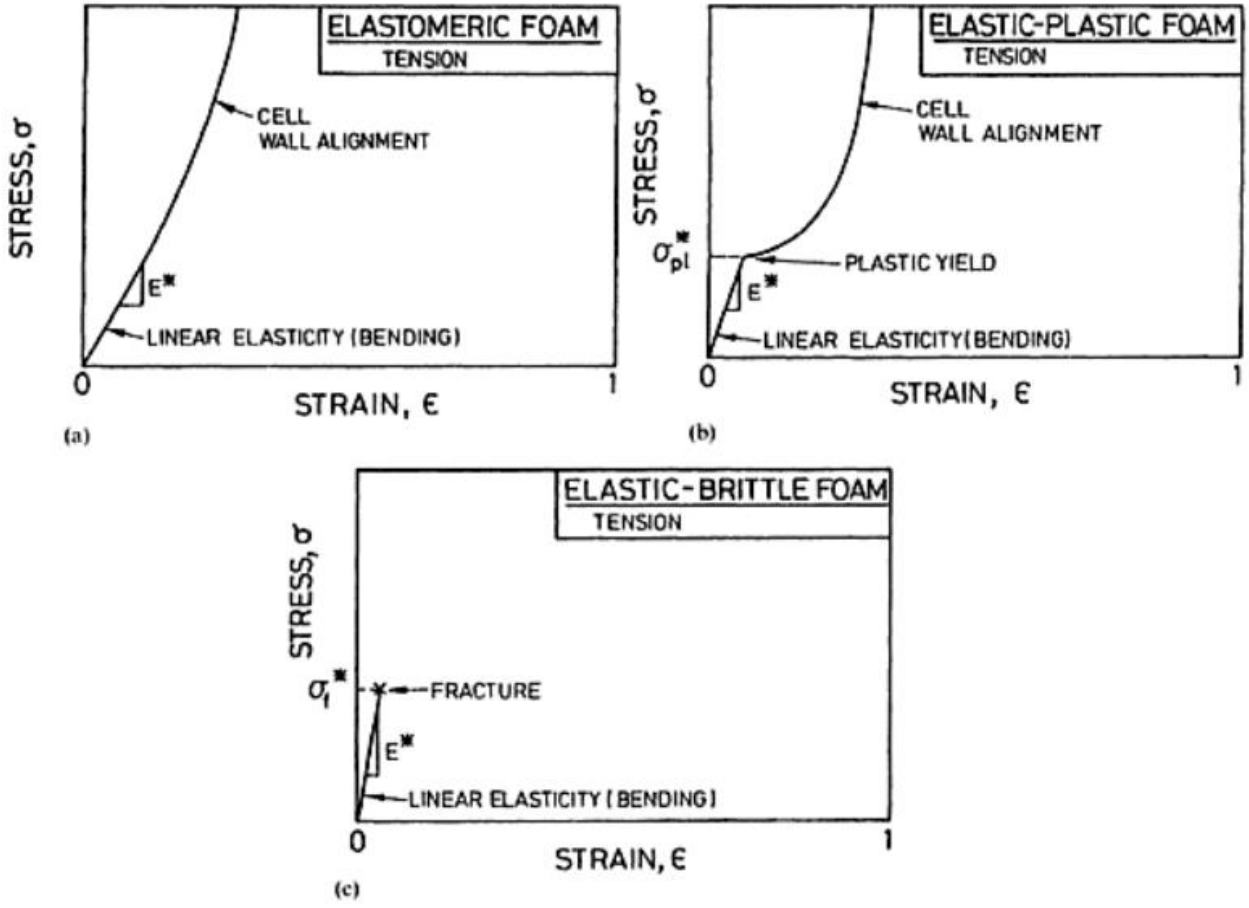

Figure 5: Mechanical stress and strain of tensile testing foams (Gibson & Ashby, 1999).
Various graphs show that elastomeric foams, elastic-plastic foams, and elastic-brittle foams have different tensile behaviors.

Upon completion of a mechanical test, data is most commonly illustrated and measured in comparison to the mechanical properties of the bread crumb. As seen in the figure above, comparing the tensile stress to strain illustrates different behaviors when materials with varying properties are tested. Bread, with a behavior best defined as a non-linear viscoelastic, is a combination of both elastic-plastic foam and elastic-brittle foam, as it illustrates a combined behavior of the two (Scanlon & Zghal, 2001). As observed in the following Figure 6, it is clear that the tensile testing of bread includes the elastic region, yet continues to experience stress which reaches a maximum before fracture ultimately occurs.

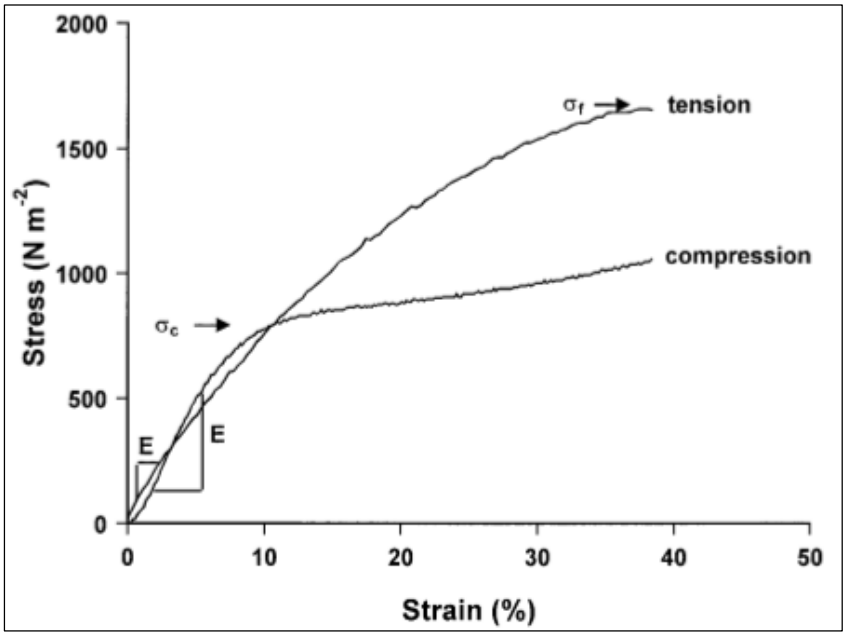

Figure 6: Typical stress and strain behavior of bread crumb under tensile and compressive loads, with maximum stresses and Young's Modulus labeled (Liu & Scanlon, 2003).

2.3.1 MECHANICAL PROPERTIES

Relative density, defined as "crumb density divided by solid density, or the density of the crumb cell walls" (Zghal, Scanlon, & Sapirstein, 2002), has an effect on mechanical properties (Gibson & Ashby, 1999). Structural homogeneity, as it relates to relative density, has a clearly displayed effect on mechanical properties of bread crumb. Other mechanical properties of bread,

such as Young's modulus and failure stress, have been found to be correlated with the density and number of cells per unit area (Zghal, Scanlon, & Sapirstein, 2002).

Additional significant mechanical properties of foams in a tensile test include yield stress, ultimate tensile strength, and relative modulus of elasticity. These values provide information on the mechanical behavior of the crumb structure in question. Strain and elongation are also investigated as mechanical properties (Gibson & Ashby, 1999).

2.4 THEORETICAL MODELING

A theoretical model is an abstract description or illustration of a process or product, which can be used to "optimize products for specific functionalities" (Wang, Karrech, Regenauer-Lieb, & Chakrabati-Bell, 2013). Creating a digital environment influenced by the honeycomb structure and application for a three-dimensional foam, for example, can be utilized in order to characterize and model bread crumb as presented in the following sections.

2.4.1 HONEYCOMB STRUCTURE

A honeycomb is used "in a broader sense to describe any array of identical prismatic cells which nest together to fill a plane" (Gibson & Ashby, 1999). These cells can consist of triangular, square, rhombic, or most commonly, hexagonal shapes. Examples of these cellular shapes can be found in Figure 7 below.

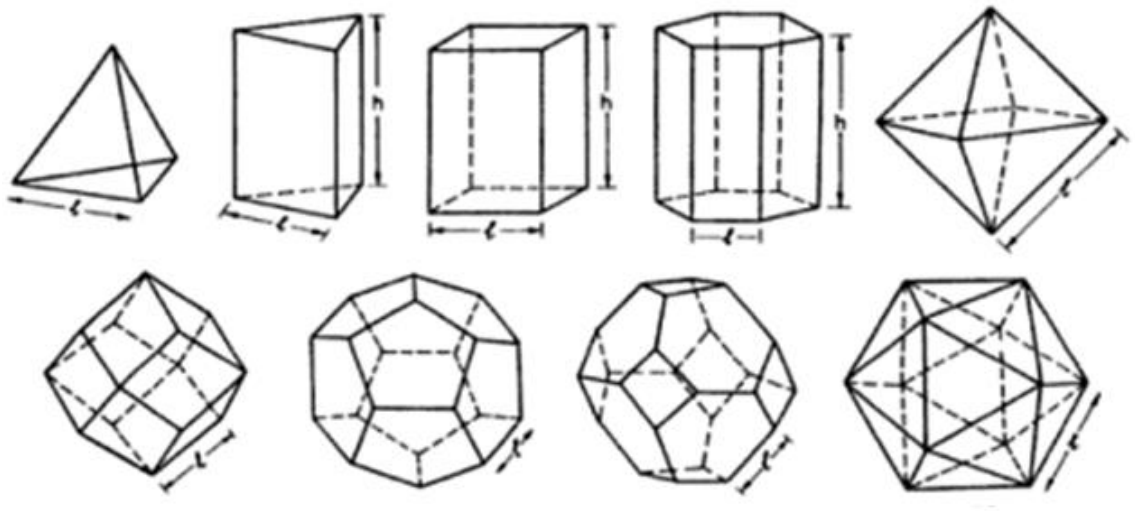

Figure 7: Various shapes for cellular solids (Gibson & Ashby, 1999).
This image illustrates the hexagonal and rhombic dodecahedral figures that are referenced in this report.

Digital modeling of honeycombs can optimize the use for different functionalities and applications. For example, the results of studying honeycombs "shed light on the mechanics of the much more complex three-dimensional foams" (Gibson & Ashby, 1999). The act of analyzing these intricate three-dimensional foams is very difficult due to the distortion that occurs during deformation. However, "because honeycombs have a regular geometry, their deformations can be analyzed more or less exactly to give equations which describe their properties" (Gibson & Ashby, 1999). As a result of honeycomb analysis, the following density equations based on shape in Table 1 below are provided by the literature in order to describe the behavior of cellular solids.

Table 1: Relative density equations by shape of cellular solid (Gibson & Ashby, 1999).

Honeycombs	
Equilateral Triangles	$\frac{\rho^*}{\rho_s} = 2\sqrt{3} * \frac{t}{l}\left(1 - \left(\frac{\sqrt{3}}{2} * \frac{t}{l}\right)\right)$
Squares	$\frac{\rho^*}{\rho_s} = 2 * \frac{t}{l}\left(1 - \left(\frac{1}{2} * \frac{t}{l}\right)\right)$
Regular Hexagons	$\frac{\rho^*}{\rho_s} = \frac{2}{\sqrt{3}} * \frac{t}{l}\left(1 - \left(\frac{1}{2\sqrt{3}} * \frac{t}{l}\right)\right)$
Three dimensions: open cells (aspect ratio A_r=*h*/*l*)	
Triangular Prisms	$\frac{\rho^*}{\rho_s} = \frac{2}{\sqrt{3}} * \frac{t^2}{l^2}\left\{1 + \frac{3}{A_r}\right\}$
Square Prisms	$\frac{\rho^*}{\rho_s} = \frac{t^2}{l^2}\left\{1 + \frac{2}{A_r}\right\}$
Hexagonal Prisms	$\frac{\rho^*}{\rho_s} = \frac{4}{3\sqrt{3}} * \frac{t^2}{l^2}\left\{1 + \frac{3}{2A_r}\right\}$
Rhombic Dodecahedra	$\frac{\rho^*}{\rho_s} = 2.87 * \frac{t^2}{l^2}$
Tetrakaidecahedra	$\frac{\rho^*}{\rho_s} = 1.06 * \frac{t^2}{l^2}$
Three dimensions: closed cells (aspect ratio A_r=*h*/*l*)	
Triangular Prisms	$\frac{\rho^*}{\rho_s} = 2\sqrt{3} * \frac{t}{l}\left\{1 + \frac{1}{2\sqrt{3}A_r}\right\}$
Square Prisms	$\frac{\rho^*}{\rho_s} = 2 * \frac{t}{l}\left\{1 + \frac{1}{2A_r}\right\}$
Hexagonal Prisms	$\frac{\rho^*}{\rho_s} = \frac{2}{\sqrt{3}} * \frac{t}{l}\left\{1 + \frac{\sqrt{3}}{2A_r}\right\}$
Rhombic Dodecahedra	$\frac{\rho^*}{\rho_s} = 1.90 * \frac{t}{l}$
Tetrakaidecahedra	$\frac{\rho^*}{\rho_s} = 1.18 * \frac{t}{l}$

While this honeycomb model of relative density calculation is not foolproof for three-dimensional foams such as bread cells, the other three-dimensional equations provided by the literature provide more accurate data. These equations inspired the process of modeling bread cells in the digital model, which is explained in the methodology in Chapter 3 of this report.

2.4.2 DIGITAL MODEL FOR BREAD CRUMB

As explained in the literature, the use of scanners, video image stills, and Magnetic Resonance Imaging (MRI) can be used to capture two dimensional imagery of bread crumb, which provide digital images. As these methods of digitizing bread crumb are limited to two dimensions, challenges are presented in creating an accurate model of bread crumb. With advanced methods, such as x-ray tomography, bread crumb can be captured in three dimensions. The digital model of bread crumb can then be analyzed with the Finite Element Method, as accomplished by several researchers and reported in Springer Science (Babin, Valle, Dendievel, Lassoued, & Salvo, 2005). This digital bread crumb has been used to replicate the structure and mechanical properties of real bread samples. Upon comparison, digital bread crumb "exhibits similarities to real products in terms of cell wall thicknesses as seen from surface appearance. Results from digital compression experiments using finite element analysis showed differences in Young's moduli between breads" (Wang, Karrech, Regenauer-Lieb, & Chakrabati-Bell, 2013), which is due to variation in both pore distribution and porosity. Nevertheless, digital bread crumb is comparable to real bread samples given the advanced software and hardware necessary to capture bread crumb on a three-dimensional level.

2.4.2.1 DEVELOPMENT OF DIGITAL MODEL

Digital bread crumb is generated by a process that begins with creating a completely solid digital mesh structure. If the structure does not meet the target porosity requirement, then a spherical pore with a random volume governed by Weibull parameters is created. This created pore is randomly placed within the solid digital mesh structure, where all the elements that fall within the sphere boundaries of the pore are removed from the solid digital mesh structure. This process repeats until the structure meets the target porosity requirement.

Once the target porosity requirement is reached, the elements that were left unconnected to other elements essentially remained dangling, and therefore are also removed. After dangling elements are removed, the porosity of the digital bread crumb structure is recalculated. Lastly, the digital bread crumb structure is finalized and the simulation of mechanical tests begins (Wang, Karrech, Regenauer-Lieb, & Chakrabati-Bell, 2013).

2.4.2.2 APPLICATION OF DIGITAL MODEL

This method is used to create random digital bread crumb based on real bread samples and their pore structure. "Digital bread crumb has been shown to be suitable for use in isolating the effects of porosity and pore structure for the simple compression of materials. Digital bread microstructures have been shown to be quantifiably similar to real world products in terms of cell wall thickness measurements, though they are not yet equivalent. Digital small strain compression experiments were performed, demonstrating significant differences in Young's moduli which can be attributed solely to differences in pore microstructure" (Wang, Karrech, Regenauer-Lieb, & Chakrabati-Bell, 2013). Although some aspects are not yet equivalent to real bread samples, future efforts to include additional properties will improve the digital bread crumb model.

CHAPTER 3: OBJECTIVES

The goal of this project was to model bread to later analyze properties including porosity and density comparable to that of physical bread. In the initial stages, the main objectives of this project were the following:

1. Develop a 3D SolidWorks model for the crumb of bread.
2. Utilize standardized foam models to develop relationships between structural parameters, density, and other mechanical properties.
3. Study the effect of structural variables on density and mechanical properties.
4. Use a 3D printed sample based on these models and compare the predictions with normalized bread properties.

After several approaches to achieve a realistic model of bread to later 3D print and determine its properties, the above objectives were deemed unfeasible. As a result, the scope of the project changed to focus on tensile testing store-bought bread and analyzing how its cellular structure changes as a function of time, force, and elongation. Taking these elements into account, the following objectives were established:

1. Develop a standardized tensile testing procedure for prepared samples of bread.
2. Follow the determined procedure and acquire footage of the sample fracture.
3. Analyze the resulting data and investigate fracture patterns and changes in the bread crumb due to the tensile test.
4. Determine the accuracy of the digital model by theoretical calculations in MATLAB and SolidWorks.

The next chapter explains the methodology and procedures followed in order to achieve the goal of analyzing data and properties of physical bread.

CHAPTER 4: METHODOLOGY

4.1 SOLIDWORKS MODEL

The purpose of creating a digital model of bread crumb was to further investigate the cellular structure in terms of its open and closed cell ratio and any potential effects that it had on mechanical properties. Modeling software is capable of applying mechanical loads to digitally created parts, which was another method to test the model and determine if results were similar to those of the experimentally tested bread crumb. By 3D printing the digital model and performing tensile tests, further results would be obtained and compared to those of the experimental results and the digital model results.

To accomplish a digital model equivalent to physical bread crumb, several requirements were deemed necessary. A random distribution of pores was required to ensure that the natural process of bread making, which forms the cellular structures, was not compromised. The additional requirements are discussed throughout this chapter.

In order to create the digital model, the software SolidWorks 2015 was initially selected. Beginning with a rectangle on the front plane, Microsoft Excel was used to generate 100 lists of three randomized numbers between the boundaries of the solid body, which were then imported into SolidWorks. These numbers represented the x- and y-coordinates and a radius *r* to be located inside the boundaries of the rectangle. Once all the coordinates were imported, the radius of each point was manually sketched in SolidWorks, and the remaining solid body was extruded to create a model for a thin layer of bread, as shown in Figure 8 below. These steps were repeated several times in order to create multiple layers, which were later assembled together in order to create both open and closed cells.

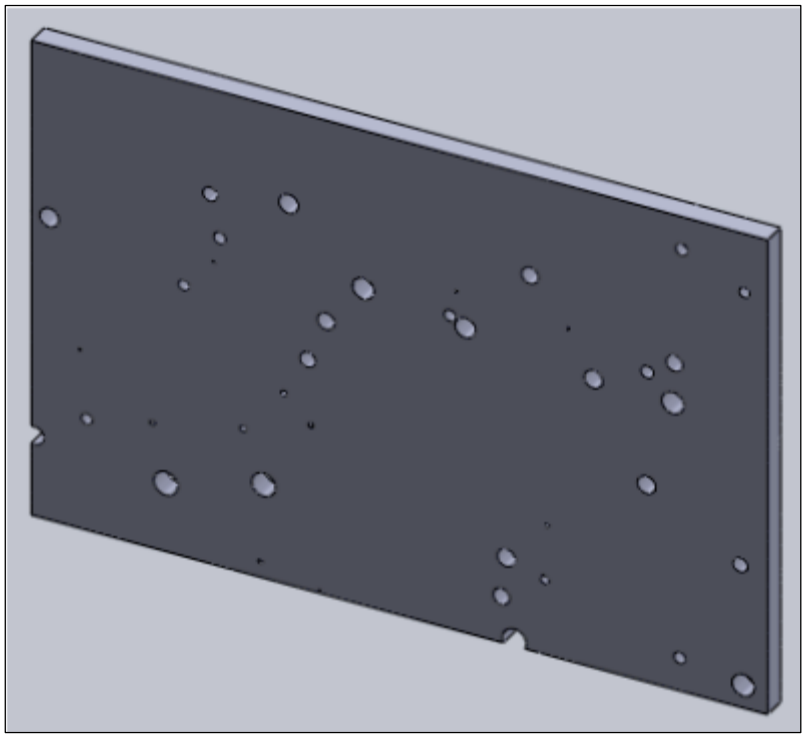

Figure 8: SolidWorks model with randomly located and sized cylindrical structures as open cells.

With intermediate levels of skill and experience within SolidWorks software, utilizing the program's full capabilities and performing a Force Analysis test on the assembly of parts was unsuccessful. The next approach was to again, start on the front plane, but to create hexagons in a more unified, honeycomb structure made up of one layer instead, as shown in Figures 9 and 10 below.

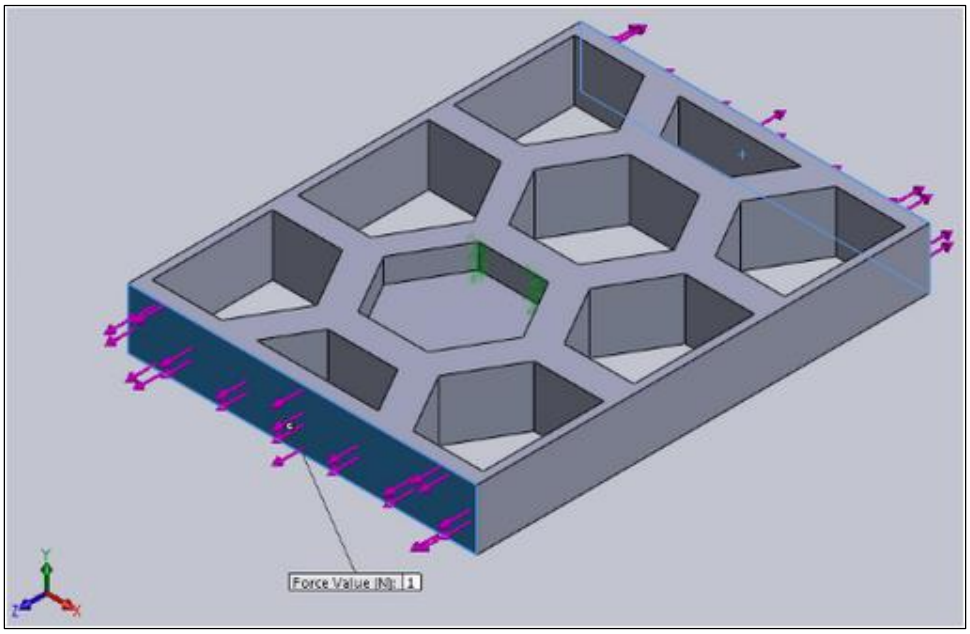

Figure 9: Hexagonal structures with both open and closed cells. This model does not include the random nature of bread crumb. The purple arrows represent the tensile load of 1N.

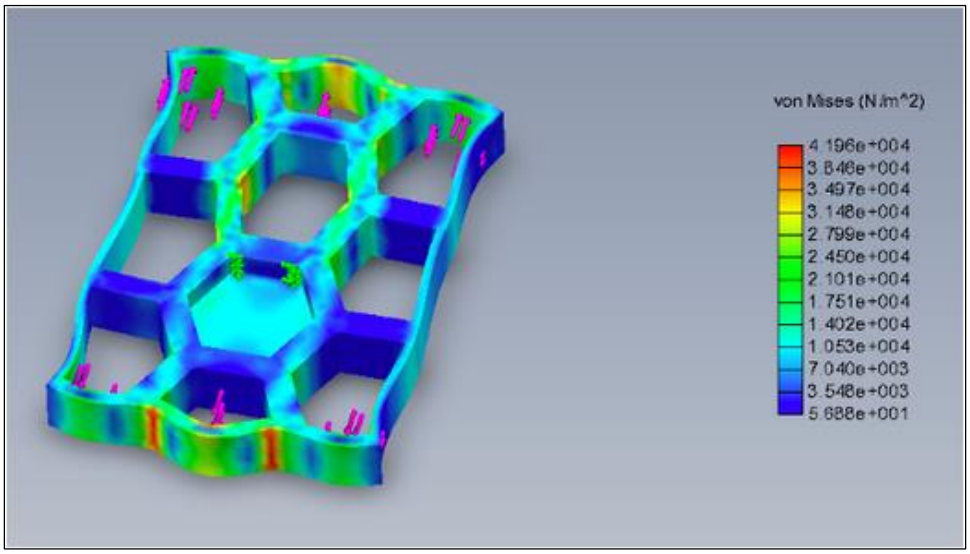

Figure 10: Resulting forces on the hexagonal structure from a 1N tensile load in SolidWorks Force Analysis.

This method of a unified honeycomb structure, as shown above, allowed for Force Analysis testing, but lacked variety and randomization due to the predictable cell placement, which is contradictory to bread crumb. For this reason, the honeycomb model was not utilized.

4.2 MATLAB CODE

After experimenting with the method of accompanying SolidWorks and Microsoft Excel, the idea of using a MATLAB code to create a SolidWorks model was presented as a more dynamic approach, better accounting for randomization of the cell locations and sizes. With the help of Siamak Ghorbani Faal, PhD Candidate at Worcester Polytechnic Institute, a code was created to convert MATLAB script into a SolidWorks STL file. A rectangular prism, or cuboid, was generated from code which required input values representative of the body's length, width, and height, as well as the centroid x-, y-, and z-coordinates. These values were pre-determined and not random, as the figure was intended to represent the crumb within a loaf of bread.

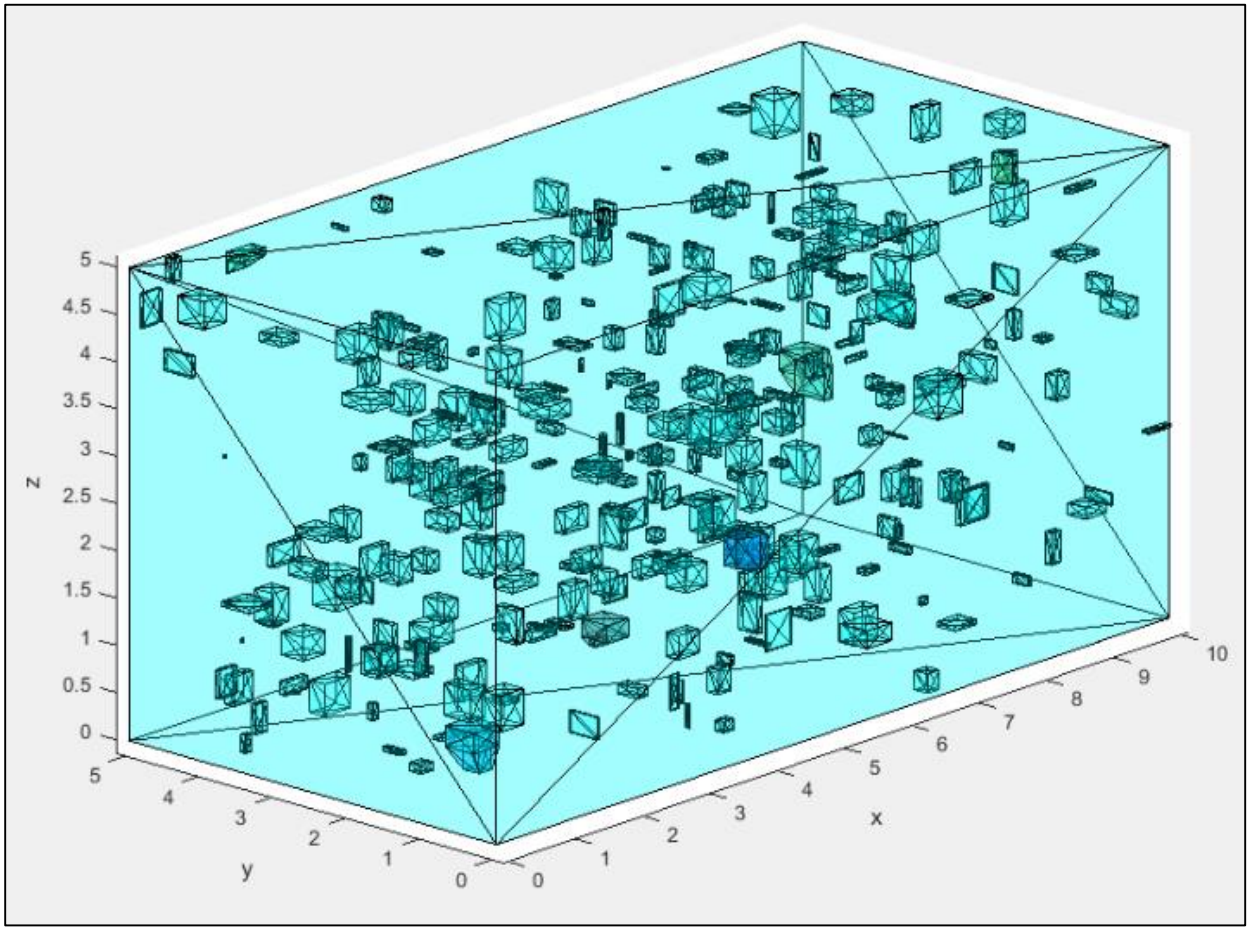

Figure 11: Initial model of an entire loaf of bread with rectangular open cells.

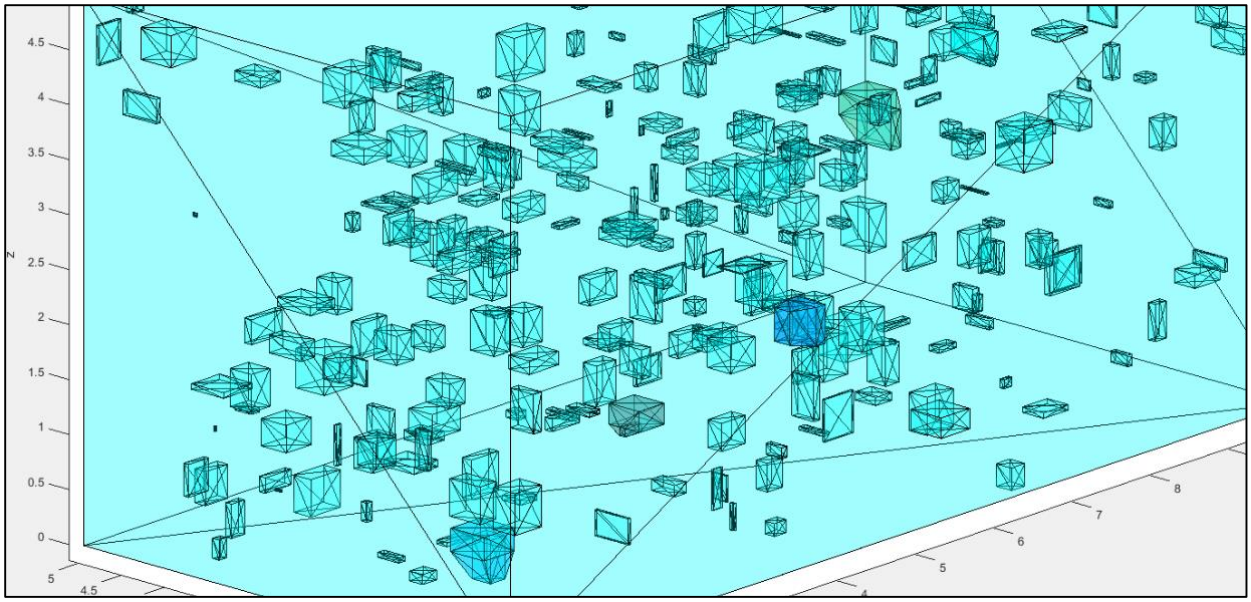

Figure 12: Closer look at the cellular structures inside of the bread model.

As apparent in Figures 11 and 12 above, the majority of the cellular structures in the model are rectangular prisms, with a small number of colliding cells creating varied structures. When undergoing changes after experiencing an applied force, either through computer modeling or physical testing, each structure would break in different ways.

Instead of generating the entirety of the bread crumb as a single solid body, the dimensions were changed in order to create a single slice of the crumb. This was done with the intention of increasing the number of open cells when multiple slices are combined together. The resulting slice from the altered dimensions is shown in Figures 13 and 14 below.

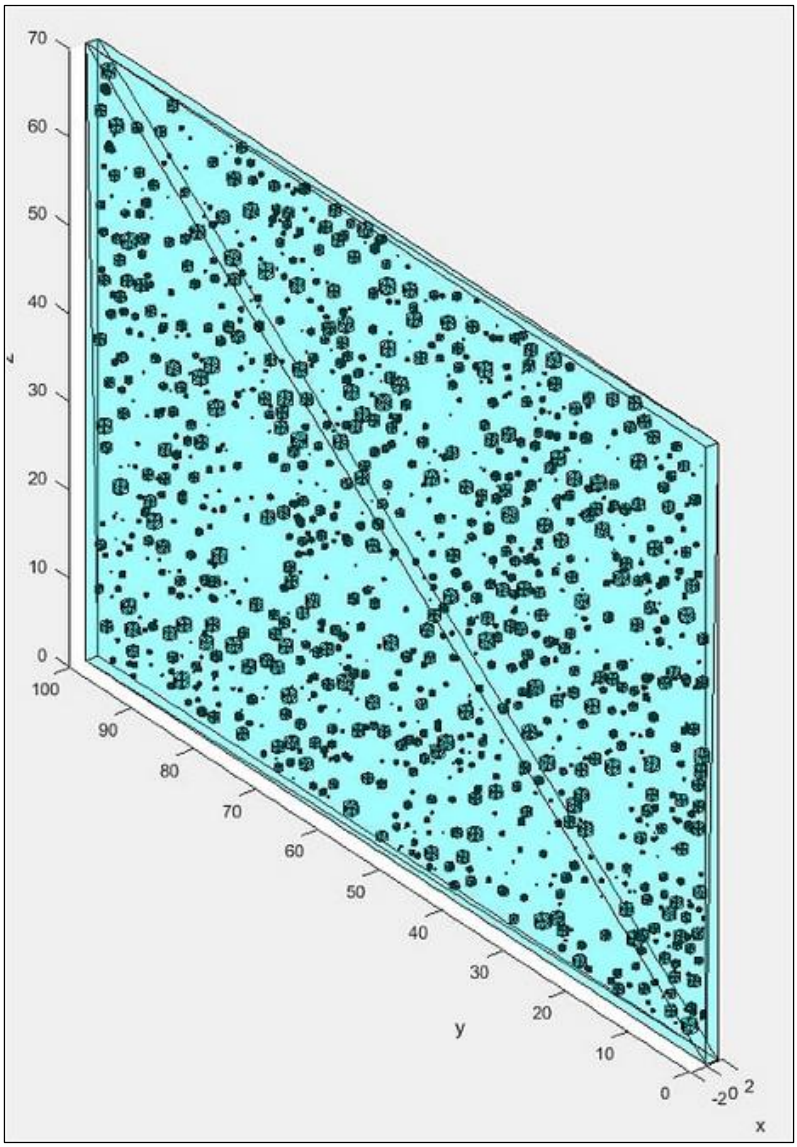

Figure 13: Single slice of bread with rhombic dodecahedral cellular bodies inside.

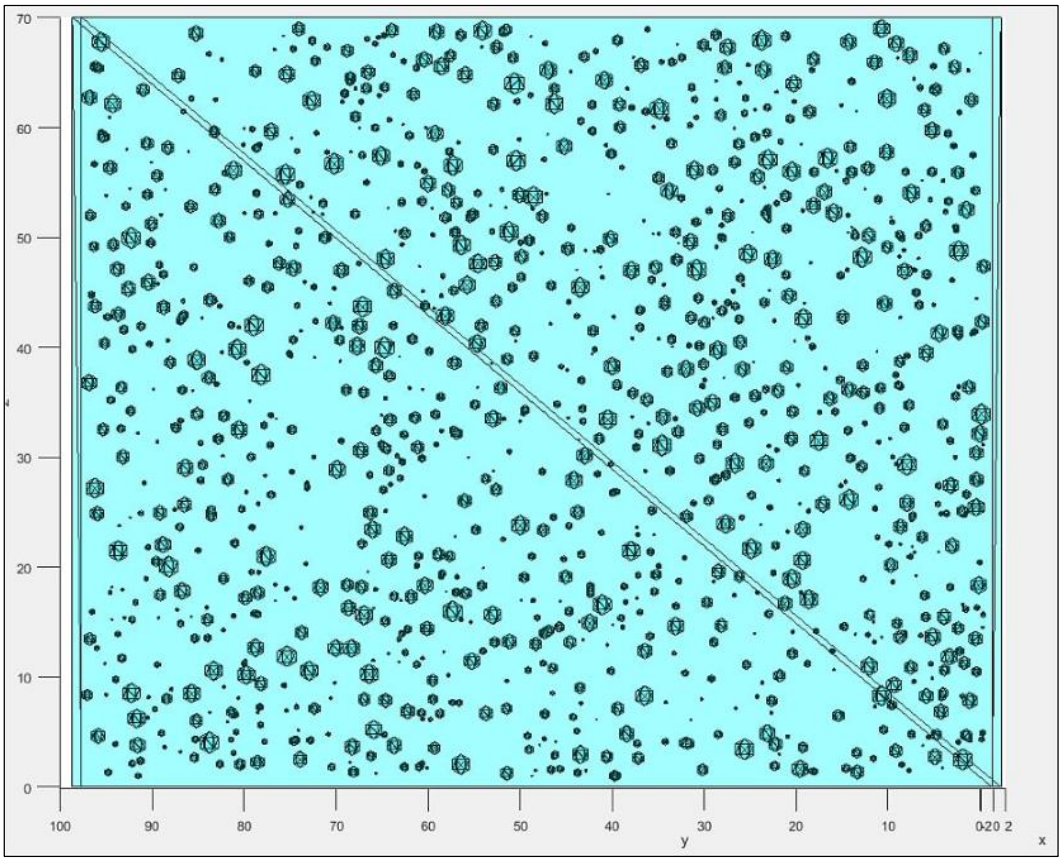

Figure 14: View from the front plane of the cellular structures inside the bread body.

Digitally modeling the bread in slices also allows for the possibility of 3D printing a model more similar in dimension to the real bread crumb samples that were used for physical testing. In generating data for these single-slice models, 100 matrices with six columns of randomly generated numbers between the boundaries of the original cuboid were combined into one matrix, which was run through the same code that created the outer boundaries. This generated randomly sized and placed cuboids, representative of the cells in bread crumb, inside the solid body. From the MATLAB model previously shown in Figures 13 and 14, the resulting SolidWorks model generated from the STL file is displayed in Figures 15 and 16 below.

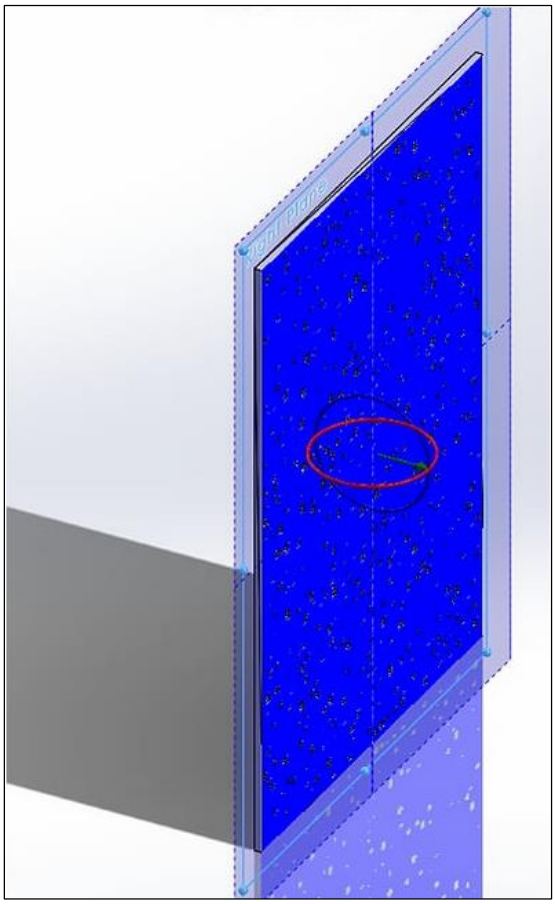

Figure 15: SolidWorks figure created from the MATLAB plots shown in Figures 13 and 14.

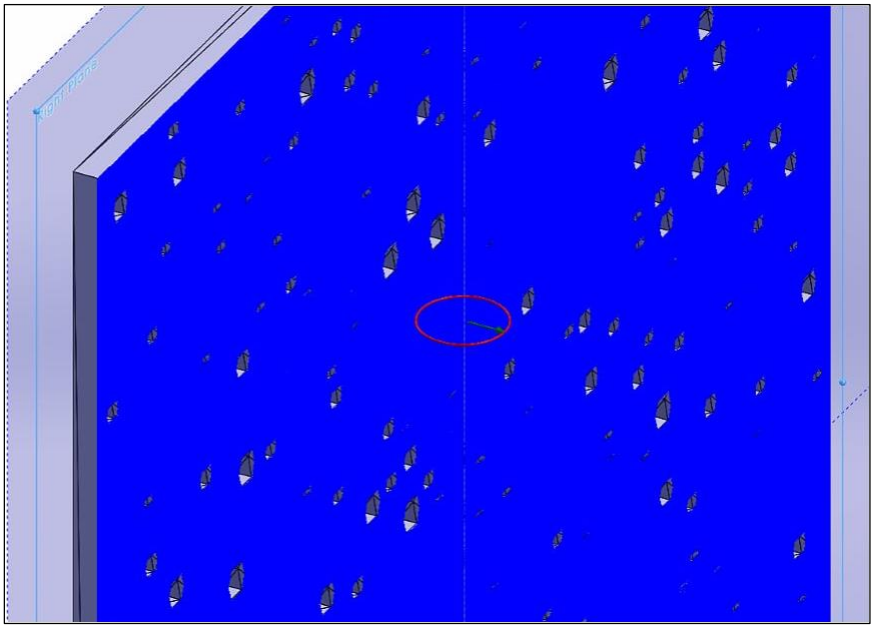

Figure 16: Closer view of the open cells in the SolidWorks solid body.

As seen in Figures 15 and 16 above, the overall blue area represents the solid body, or the closed cells in the model. Each cellular structure generated by the MATLAB code becomes an open cell when the file is opened in SolidWorks, which is indicated by the open cells in the cross-sectional area of the model.

4.2.1 Random Distribution of Cells

With a random distribution of cells in the model, it was possible for the cells to overlap or collide with one another. This would eventually cause an error when turning the MATLAB code into an STL file. The software includes an existing function which utilizes the concept of Delaunay triangles, and creates a Delaunay triangulation when given a list of connected points (The MathWorks, Inc., 2015). In this case, the list of connected cuboids consisted of cells which overlapped or collided. As a result, an additional function, found in Appendix E, was included in the code in order to create cells made up of the same dimensions of the outermost points of the connected cells. Figure 17 below shows an example of a cell made up of several overlapping or colliding cells.

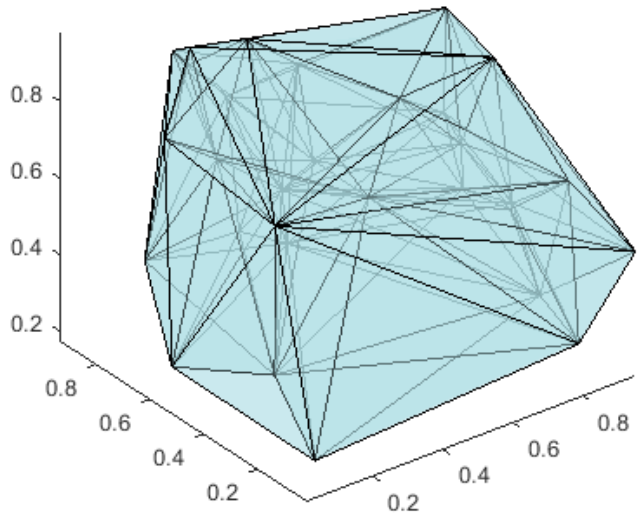

Figure 17: Delaunay Triangulation.
This illustrates the result of the function existing in MATLAB to combine multiple bodies into one solid body.

The Delaunay Triangulation is utilized frequently in the MATLAB code and is evident in the previous Figures 11 and 12, as there are several cellular structures that are not rectangular prisms in that version of the MATLAB code.

4.2.2 Volume and Density

Another requirement of the MATLAB code was to ensure that all cells were in the range of the accepted cell size, which as mentioned in Chapter 2, is between 1.23 mm and 2.00 mm (Wang, Austin, & Bell, It's A Maze: The Pore Structure of Bread Crumbs , 2011). With the previous code to combine cells, there became the possibility of cells exceeding or falling short of the accepted range. An additional function, found in Appendix F, was then created in order to perform a volume check on each cell. This would remove any combined cells that exceeded the limit. In order to perform density calculations, both mass and volume values would be necessary. As the model is solely digital, no mass value is present and as a result, density cannot be addressed.

4.2.3 Open and Closed Cell Ratio

The MATLAB code was updated in order to calculate the variable “total volume”, found in Appendix E, which calculates the total volume taken up by the cells that filled the original solid body. As a result of the code’s randomization of cell size and location, as well as the ability to alter the initial number of cells present in the structure, the open-closed cell ratio of the model was theoretically different each time the code was run. In order to get an overall estimate, the code was run 10 times to gather an average of the open-closed cell ratio with the initial number of cells at a value of 2,000. Multiple MATLAB codes are referenced in Appendices E through L, and the resulting values and data are further discussed in Chapter 5.

4.3 TENSILE TESTING BREAD

Numerous tensile testing trials were performed in order to become familiar with the technique and to determine the best practices for sample preparation and testing procedures. The Instron Series 4200 and 4300 Control Console, as shown in Figure 18 below, were used for testing.

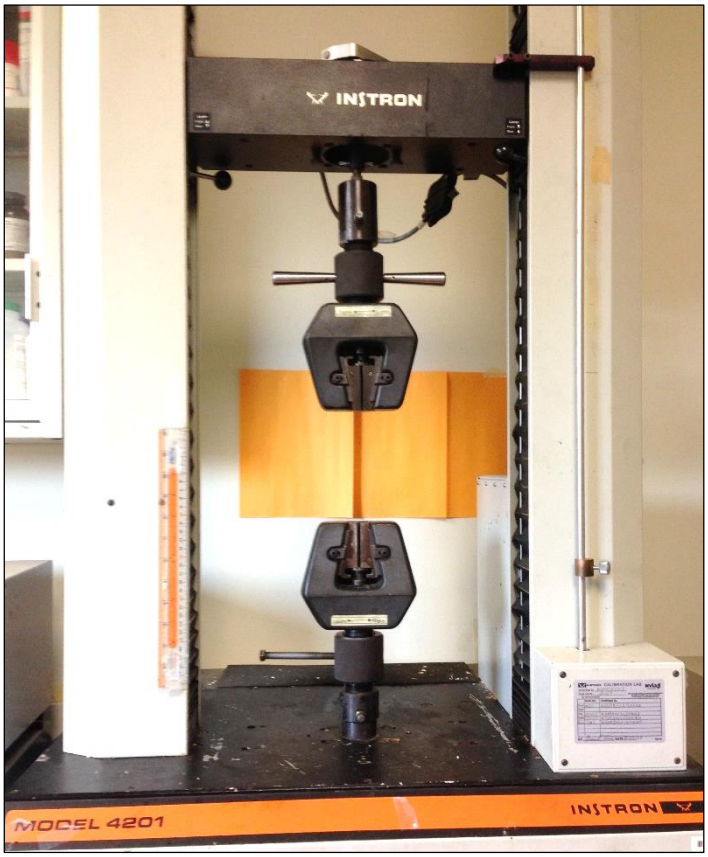

Figure 18: Instron Model 4201 used for tensile testing.

The console provided the force, time, and specified crosshead speed throughout the tests. This raw data was extracted through the console and entered into Microsoft Excel for further calculation. Once the initial trials were complete, a specific procedure was created for the subsequent sets of data for analysis.

Bread samples were prepared by a series of steps. First, a chef's knife was sharpened in order to cut the crust off of the bread by sliding the edge along the bread's surface while applying

minimal downward pressure on the bread crumb. Each slice, with a thickness of approximately 1.5 cm, yielded two 3” x 2” samples. Two slices of cardboard were cut roughly the same size as the samples. One side of each cardboard slice was ripped roughly 1” deep, into two halves, where super-glue was then applied. The ends of the bread samples were inserted into the super-glued cardboard and set to dry. This method of preparation was chosen over inserting the slices of bread into the grips of the Instron machine in order to avoid compressing the ends and compromising the bread crumb. A sample prepared by the above procedure is shown in Figure 19 below.

Figure 19: Example of a bread sample for tensile testing. Note the dimensions.

4.3.1 INITIAL TRIALS

In the early stages of testing, three trials of testing 20 samples each were performed. Sample preparation was split between project partners, with 10 samples each. In the first initial trial, a Sony HDR-XR500 video camera was used to record the first 10 samples during the tensile test, and a Casio EXILIM 12.5X camera was used to record the second 10 samples. This was to determine which camera would best suit the projects’ needs in terms of media quality. A

comparison of the quality from each device is shown in the following combination of images in Figure 20, with the camera quality on the left and the video camera quality on the right.

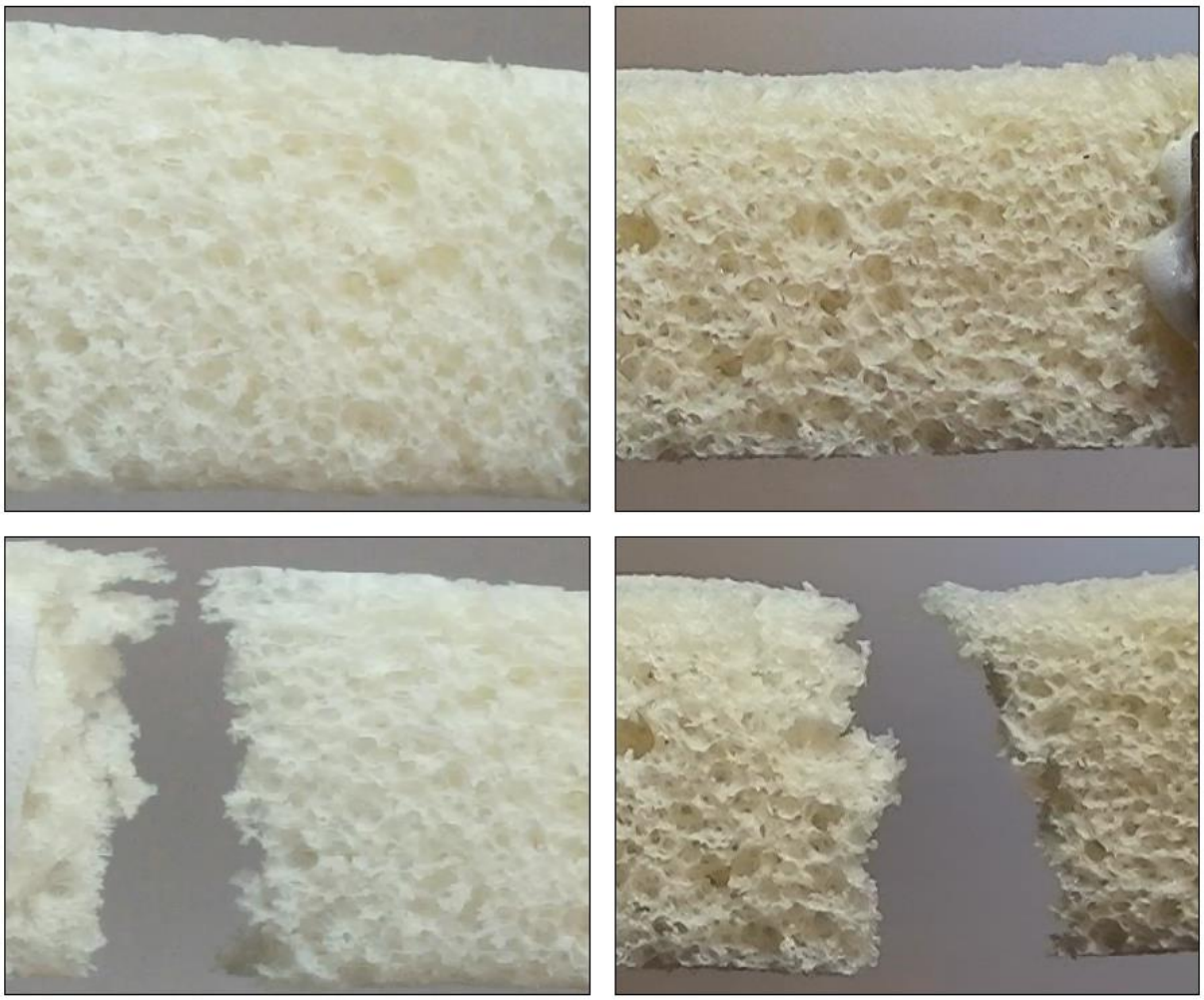

Figure 20: Comparison of the video camera and camera footage to determine the best quality image. Camera-quality stills are on the left, while video camera-quality stills are on the right.

It was determined that the Sony HDR-XR500 video camera yielded the clearest image. For the second initial trial, the same video camera was used and the focus was on improving skills both during recording, and with video editing software afterwards, in order to create videos that support initial predictions and existing literature. The final trial before creating a standardized procedure was the most extensive of the initial trials. The trial involved microscopic photography of the bread crumb prior to tensile testing in order to acquire the cell wall thicknesses, cell shape,

cell size, and open-closed cell ratio. The microscope used was AmScope Model IN300TB at the minimum magnification of 4x, in addition to ToupView camera software. After the preliminary photos were taken, the tensile test was recorded with the video camera, focusing deeper on the area of fracture. Finally, the microscope was used again to analyze the crumb along the fracture zone in order to determine trends and patterns. This particular trial inspired the standardized procedure.

4.3.2 STANDARDIZED PROCEDURE

Over the course of one week, four sets of 10 samples were prepared for testing, in addition to two extra samples within the fourth set, due to one remaining slice of bread. All samples were prepared from the same loaf of store-brand white bread to allow for the investigation of any potential changes in data as a result of staling. Photos were taken on alternating days throughout the week, with the exception of the first and final days of the trials, which were taken on the same days as testing. A photograph of 10 samples directly after testing can is shown in Figure 21 on the right.

Figure 21: Post-fracture samples prepared for microscopic analysis.

The standardized procedure of these trials followed the methodology of the final preliminary trial above, including the microscopic photos and video recording. After the final day

of testing, the acquired data for each fracture of the 42 samples consisted of microscopic photos before testing, video recordings during testing, microscopic photos after testing, and the data provided by the Instron machine. To prepare data for analysis, videos taken with the Sony HDR-XR500 video camera were edited to best illustrate the properties as described in the objectives of this project. A photograph displaying the final setup for the standardized procedure is shown in Figure 22 below.

Figure 22: Final setup for tensile testing of bread samples and recording the tensile data.

CHAPTER 5: RESULTS AND DISCUSSION

With the intention to digitally model bread and later analyze properties compared to that of physical bread, a better understanding of the crumb was acquired. As described in the previous chapter, after several approaches, the scope of the project progressed and a deeper analysis into the change in cells as a function of time, force, and elongation developed. This chapter briefly presents the results from the initial digital modeling, then includes data analysis, and provides the mechanical and structural findings that became evident from tensile testing and microscopic investigating through analytic calculation as well as graphical examination.

5.1 MATLAB MODELING

The MATLAB code was executed 10 times to provide 10 random sample data, figures, and SolidWorks parts. After execution of the code, the model was displayed in a 3D figure, as shown in Figure 23 on the right. The relevant variables generated along with the model can be seen in Table 2 below.

As evident in the figure, there is a substantial number of cellular structures present in the overall model of the sample, yet there still remains a significant amount of the light blue, which represents the solid body. This model has a much greater closed cell presence than that of open cells, which is unrealistic in bread modeling. The values can also be found in Table 2 below.

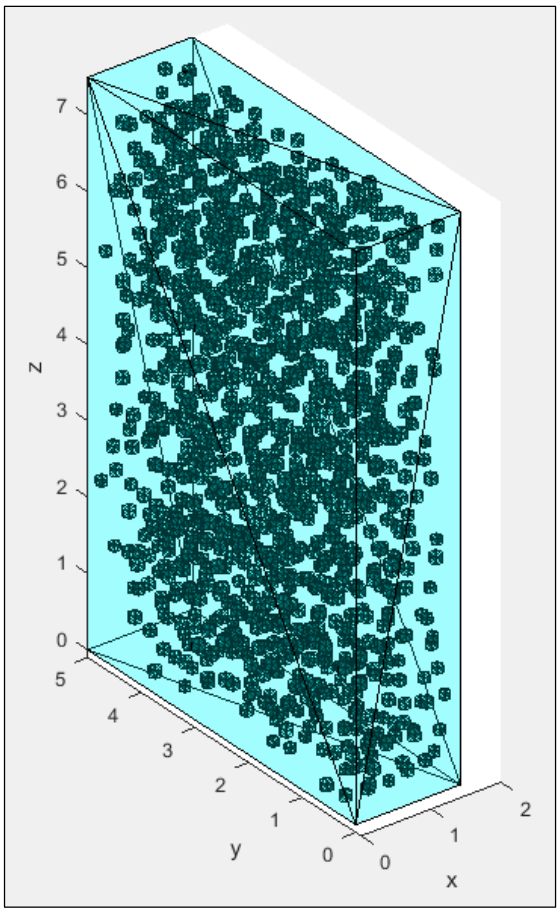

Figure 23: MATLAB model with the dimensions of one tensile test specimen as utilized in experimental data, with an open-cell count of 2,000.

Table 2: MATLAB generated values of the finalized model.

Sample #	Single Bodies	# Collisions	Total Bodies	Total Cell Volume	OPEN CELL %
1	738	402	1140	2.17	3.85
2	714	436	1150	2.20	3.90
3	787	490	1177	2.22	3.95
4	749	404	1153	2.22	3.94
5	727	425	1152	2.17	3.85
6	737	408	1145	2.15	3.82
7	769	412	1181	2.25	4.01
8	765	387	1152	2.19	3.90
9	752	416	1168	2.22	3.95
10	757	398	1155	2.19	3.88
AVG	750	418	1157	2.20	3.91

The code initially generated 2,000 cellular figures inside the 1.5 cm x 5 cm x 7.5 cm rectangular figure of the sample, which was the same size of the physical bread samples for tensile testing. When generating models, the total number of cellular structures decreased as a result of collisions yielding combined figures, as well as the removal of any volumes exceeding the maximum limit.

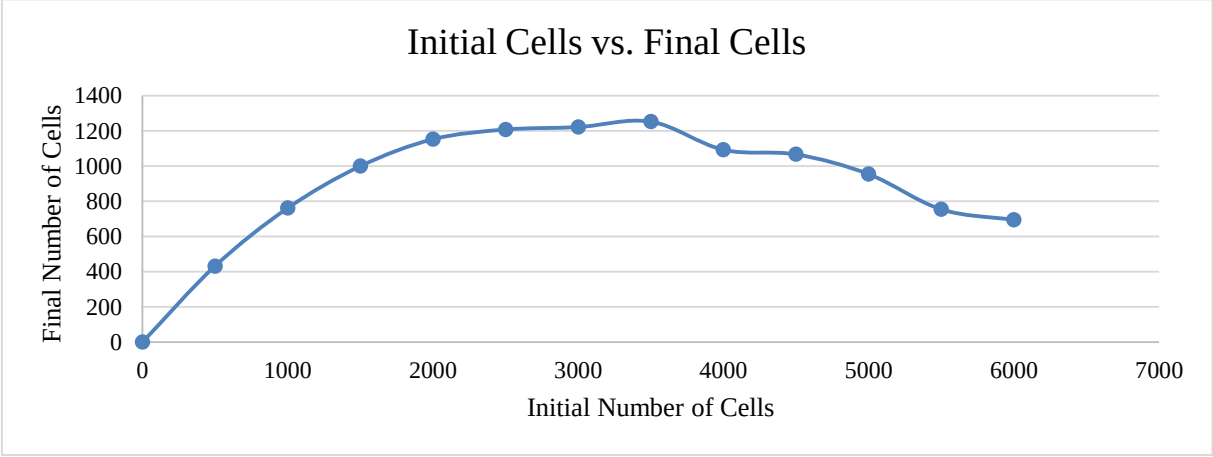

Figure 24: Initial open-cells compared to the final number of cells after collisions are accounted for.

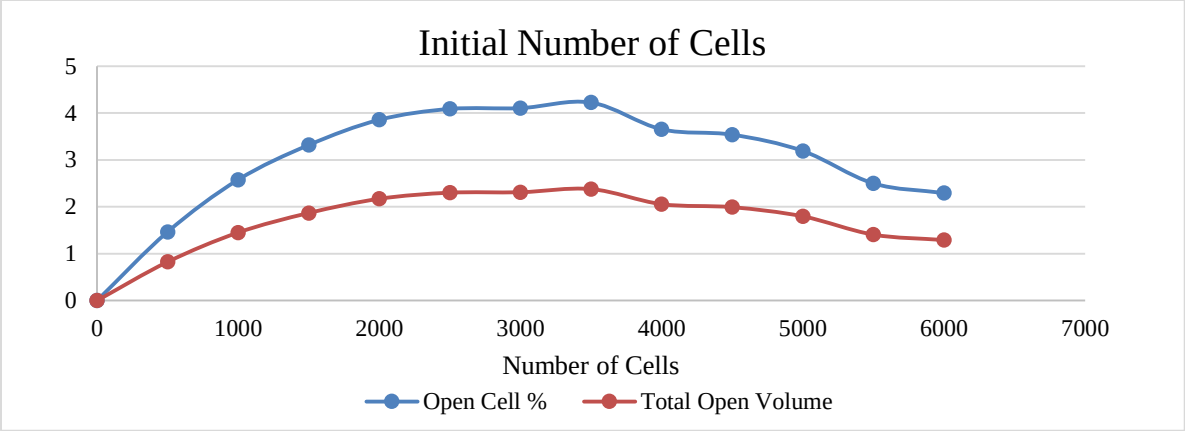

Figure 25: Initial number of open-cells compared to the overall Open Cell Percentage and the Total Open Volume (cm^3) of the solid sample.

As illustrated in Figures 24 and 25, as the number of initial cellular figures increased, the total volume remained roughly the same, as an increase in collisions increased cell volumes beyond the maximum limit more frequently. The total number of solid bodies, or open cells, in the 10 generated samples can be found in the following Figure 26.

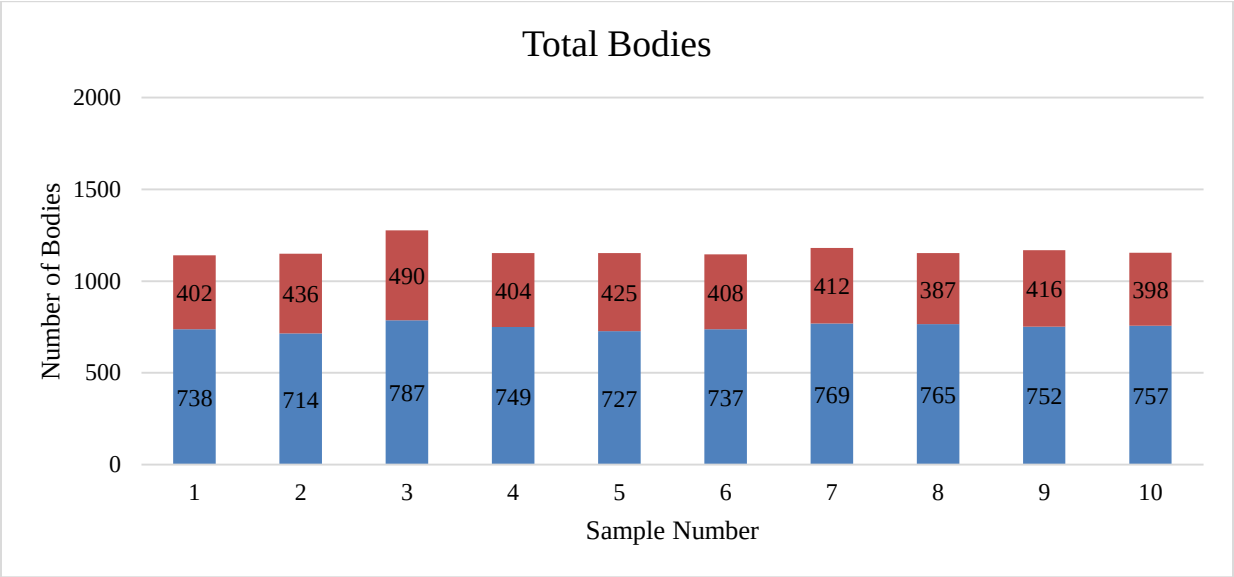

Figure 26: Total cellular bodies present in the samples. This accounts for open cells in the structure.

The average volume of the cellular bodies inside the sample was 2.20 cm^3. With the total volume of the sample of 56.25 cm^3, the open cells account for 3.9% of the total volume. This open-closed cell ratio of roughly 4% to 96% was not comparable to the ratio of 78.2% to 21.8% as

provided by the literature (Wang, Austin, & Bell, It's A Maze: The Pore Structure of Bread Crumbs , 2011). As a result, this model was deemed unrealistic, which contributed to the change in scope of the project and increased the focus on the tensile testing of bread.

5.2 Analytical Analysis

The following table is comprised of properties of 12 samples, including three samples that represent each of the four days of tensile testing. These samples were selected as they yielded the clearest videography and photography for assessment and discussion. The majority of the measured and calculated values found in Table 3 below were essential in determining the density of the sample of bread, which is crucial in order to perform mechanical properties calculations of foam structures. The calculated density listed below is the foam density, ρ^*, which was used to calculate relative density for mechanical property analysis, as discussed in the next section of this chapter.

Table 3: MagniSci data of experimental samples.

Sample	l (cm)	t (cm)	w (cm)	A_c (cm^2)	m (g)	v (cm^3)	ρ^* (g/cm^3)
D1S3	7.5	1.2	3.5	4.2	5.59	31.5	0.1774
D1S4	7.4	1.2	3.4	4.08	5.84	30.192	0.1934
D1S10	7.1	1.3	3	3.9	5.68	27.69	0.2051
D3S5	7.4	1.3	3.2	4.16	5.10	30.78	0.1656
D3S7	7	1.3	3.4	4.42	4.97	30.94	0.1606
D3S10	6.9	1.2	3	3.6	5.90	24.84	0.2375
D5S4	7.7	1.2	3.1	3.72	5.75	28.644	0.200
D5S5	7.5	1.2	3.2	3.84	5.80	28.80	0.2013
D5S10	7.1	1.2	3.2	3.84	6.43	27.264	0.2358
D7S3	7.4	1.3	3.5	4.55	5.20	33.72	0.1542
D7S6	7	1.3	3.5	4.55	4.63	32.06	0.1444
D7S11	7.6	1.3	3.6	4.68	4.78	33.35	0.1433
AVG	7.3	1.25	3.3	4.125	5.4725	29.982	0.1849

In addition to density calculations, MagniSci software was used in order to examine microscopic images of the bread crumb of each sample. The values recorded by the software were averaged by the best samples of each day and are presented in Table 4 below.

Table 4: MagniSci data summarized by daily averages.

	OVERALL %		**OPEN CELL DIAMETER (µm)**			**CLOSED CELL THICKNESS (µm)**		
SAMPLE #	Open Cells	Closed Cells	Average Horizontal	Average Vertical	Combined Average	Average Horizontal	Average Vertical	Combined Average
DAY 1	53.43	46.57	76.39	73.36	74.88	36.94	38.18	37.65
DAY 3	62.16	37.76	75.61	73.99	74.80	42.19	38.79	39.24
DAY 5	48.91	51.09	81.65	79.13	80.39	57.35	53.26	55.30
DAY 7	46.93	53.07	77.52	77.33	77.43	52.63	49.44	51.04
AVG	52.86	47.12	77.79	75.95	76.87	47.28	44.92	45.81

Complete MagniSci data for each sample can be found in Appendices A through D.

In regard to the open cells, the average diameters are comparable and account for more than half of the cellular population in bread crumb. Closed cell thicknesses have a slightly larger range than those of open cells, with significantly smaller measurements. The software was only capable of measuring the samples in the x- and y-directions, not accounting for differences in cell shape. As displayed in the table above, the average open and closed cell ratio of the bread crumb was between 52.86% and 47.12%.

Through the examination of over 200 microscopic images of bread crumb, the cellular shapes found were most accurately described as a combination of hexagonal prisms and rhombic dodecahedra. Both cellular shapes, in addition to microscopic images of the bread crumb, are shown below in Figures 27 and 28. The similarity in cellular shape is marked on the microscopic photos displayed in Figure 28 in order to highlight these cellular shapes.

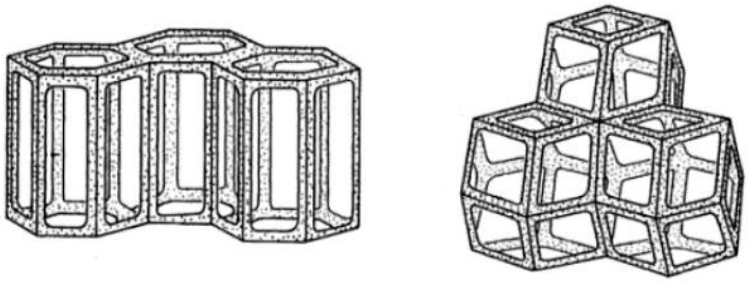

Figure 27: Hexagonal prisms and rhombic dodecahedral prisms, as established cellular solids (Gibson & Ashby, 1999).

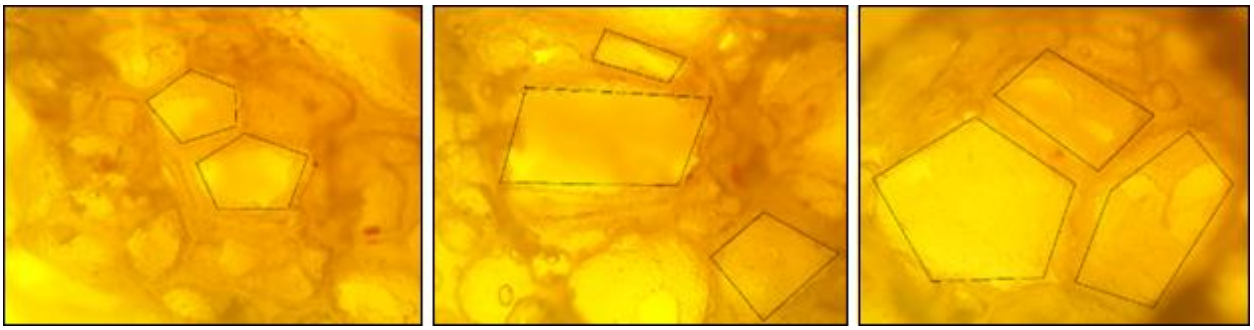

Figure 28: Illustration of hexagonal prisms and rhombic dodecahedral prisms as found in microscopic analysis of bread crumb.

From both these findings and an understanding of the natural bread cell formation process, it was determined that the behavior of bread crumb cannot be described simply by using equations relevant to honeycomb structures and hexagonal prisms. Instead, it was concluded that utilizing a combination of equations for cellular structures would create the most accurate descriptions. This results in an imperfect stacking of cells, yielding thicker cell walls, as seen previously in Table 4 above. The software provided image analysis limited to two dimensions, resulting in potential assumptions of the prismatic figures presented.

5.2.1 MECHANICAL PROPERTIES

With the calculated averages of bread density, or what is referred to as foam density, the relative and solid density can be calculated. These values were solved for and entered into Table 5 by use of the following equations:

For open celled hexagonal prisms: $\frac{\rho^*}{\rho_s} = \frac{4}{3*\sqrt{3}} * \frac{t^2}{l^2} * \left[1 + \frac{3}{2*\left(\frac{h}{l}\right)}\right]$

For open celled rhombic prisms: $\frac{\rho^*}{\rho_s} = 2.87\frac{t^2}{l^2}$

For closed celled hexagonal prisms: $\frac{\rho^*}{\rho_s} = \frac{2}{\sqrt{3}} * \frac{t}{l} * \left[1 + \frac{\sqrt{3}}{2*\left(\frac{h}{l}\right)}\right]$

For closed celled rhombic prisms: $\frac{\rho^*}{\rho_s} = 1.90\frac{t}{l}$

Table 5 below illustrates the differences in relative density with regard to cellular structure. If the bread were to be formed of entirely hexagonal prisms, the relative density would be greater than that of entirely rhombic dodecahedra. A 50/50 combination of these structures yields relative open and closed cell densities that provide a relative density with increased accuracy. In the instance of an aspect ratio, $A_r = \frac{h}{l}$, where h is the height and l is the base of the cellular prism, roughly equivalent to 1, which is the case with the data presented, the typical constants C2 and C3 lie between 1.06 and 4.61 for open cells and between 1.18 and 4.46 for closed cells (Gibson & Ashby, 1999). The constants C1, C2, and C3 were calculated with the following equations presented:

For low density honeycombs: $\frac{\rho^*}{\rho_s} = C1 * \frac{t}{l}$

For open celled foams: $\frac{\rho^*}{\rho_s} = C2 * \left(\frac{t}{l}\right)^2$

For closed cell foams: $\frac{\rho^*}{\rho_s} = C3 * \frac{t}{l}$

The values calculated and presented in Table 5 below are in accordance with these constants.

Table 5: Calculation of constants for cellular structures.

Day 1, 53.43% Open - 46.57% Closed	**t (cm)** 0.00376	**h (cm)** 0.00733	**l (cm)** 0.00763	
Cell Structure, Dimension	**ρs (g/cm3)**	**ρ* (g/cm3)**	**ρ*/ρs**	**Constant**
Open Cell Hexagon Honeycombs, 2D	0.2585	0.19201	0.742773	1.507176 C1
Open Cell Hexagon Prisms, 3D	0.40087	0.19201	0.4789778	1.972109 C2
Open Cell Rhombic Dodecahedra, 3D	0.27545	0.19201	0.697054	2.87 C2
Closed Cell Hexagonal Prisms, 3D	0.17742	0.19201	1.0822082	2.19593 C3
Closed Cell Rhombic Dodecahedra, 3D	0.20505	0.19201	0.9363665	1.9 C3
Overall Open Cell Density, 3D		0.588015917		2.421054 C2
Overall Closed Cell Density, 3D		1.00928733		2.047965 C3
Day 3, 61.16% Open - 37.76% Closed	**t (cm)** 0.00392	**h (cm)** 0.00739	**l (cm)** 0.00756	
Cell Structure, Dimension	**ρs (g/cm3)**	**ρ* (g/cm3)**	**ρ*/ρs**	**Constant**
Open Cell Hexagon Honeycombs, 2D	0.24403	0.18757	0.768608	1.481032 C1
Open Cell Hexagon Prisms, 3D	0.35719	0.18757	0.525119	1.949742 C2
Open Cell Rhombic Dodecahedra, 3D	0.24266	0.18757	0.7729699	2.87 C2
Closed Cell Hexagonal Prisms, 3D	0.16605	0.18757	1.1295642	2.17656 C3
Closed Cell Rhombic Dodecahedra, 3D	0.19022	0.18757	0.9860387	1.9 C3
Overall Open Cell Density, 3D		0.649044473		2.409871 C2
Overall Closed Cell Density, 3D		1.05780143		2.03828 C3
Day 5, 60.17% Open - 39.83% Closed	**t (cm)** 0.006	**h (cm)** 0.007913	**l (cm)** 0.00816	
Cell Structure, Dimension	**ρs (g/cm3)**	**ρ* (g/cm3)**	**ρ*/ρs**	**Constant**
Open Cell Hexagon Honeycombs, 2D	0.2291	0.20524	0.8958684	1.322694 C1
Open Cell Hexagon Prisms, 3D	0.22811	0.20524	0.8997359	1.961307 C2
Open Cell Rhombic Dodecahedra, 3D	0.15589	0.20524	1.3165927	2.87 C2
Closed Cell Hexagonal Prisms, 3D	0.13858	0.20524	1.4809801	2.186575 C3
Closed Cell Rhombic Dodecahedra, 3D	0.15949	0.20524	1.2868809	1.9 C3
Overall Open Cell Density, 3D		1.108164297		2.415653 C2
Overall Closed Cell Density, 3D		1.398786371		2.065221 C3
Day 7, 49.77% Open - 50.23 % Closed	**t (cm)** 0.0051	**h (cm)** 0.007733	**l (cm)** 0.00775	
Cell Structure, Dimension	**ρs (g/cm3)**	**ρ* (g/cm3)**	**ρ*/ρs**	**Constant**
Open Cell Hexagon Honeycombs, 2D	0.19251	0.17003	0.8832655	1.341664 C1
Open Cell Hexagon Prisms, 3D	0.20356	0.17003	0.8353114	1.927319 C2
Open Cell Rhombic Dodecahedra, 3D	0.1367	0.17003	1.243875	2.87 C2
Closed Cell Hexagonal Prisms, 3D	0.11973	0.17003	1.420123	2.157141 C3
Closed Cell Rhombic Dodecahedra, 3D	0.13594	0.17003	1.2508379	1.9 C3
Overall Open Cell Density, 3D		1.039593185		2.398659 C2
Overall Closed Cell Density, 3D		1.331998964		2.023282 C3

With the calculated relative density, it became possible to determine the relative modulus of elasticity using the following equations:

$$E = k * \left(\frac{\rho^*}{\rho_s}\right)^2$$

$$\frac{E^*}{E_s} = C1 * \left(\frac{\rho^*}{\rho_s}\right)^2$$

where *k=1* in accordance with the literature (Gibson & Ashby, 1999). In the instance of a foam, the elasticity of the foam is referenced in the well-known definition of elastic modulus:

$$E^* = \frac{\sigma}{\varepsilon}$$

Furthermore, Young's modulus was also calculated as a result of the graphical data from tensile testing bread samples. The mechanical properties previously presented in Table 5 are compared by daily results and illustrated in the following Figures 29 and 30.

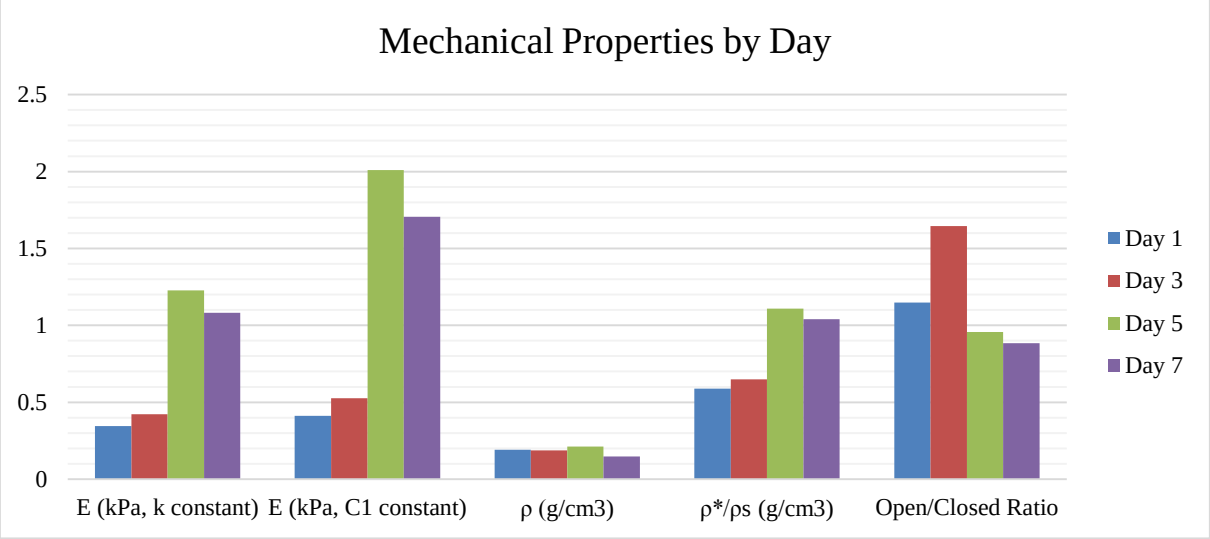

Figure 29: Mechanical properties of tensile tested bread crumb by daily comparison.

As evident in Figure 29, there appear to be daily trends in regard to elastic modulus and relative density, yet the foam density or open-closed cell ratio do not appear to follow a similar

pattern. The elastic modulus and relative density appear to increase in value as the bread stales. The measured density remains steady while the bread continues to stale for a period of one week.

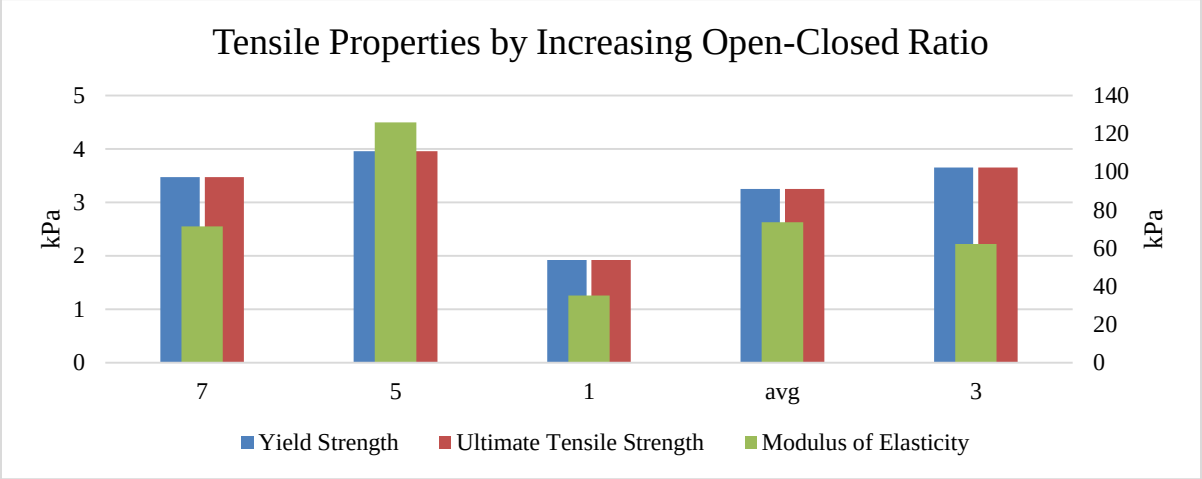

Figure 30: Tensile properties by increasing open-closed cell ratio, from left to right.

With daily values listed in order from lowest open-closed ratio to highest, it appears that there is a slight trend in data. Given that the method of obtaining the open-closed cell ratio was acquired by analyzing many two-dimensional images and considering potential error, there is the possibility that Day 3 has an open-closed cell ratio below that of Day 1, which would create a relatively uniform distribution pertaining to yield and ultimate tensile strengths. This would suggest that between Day 3 and Day 7, the bread crumb reaches a texture and structure that requires the greatest force to fracture. Given that the sample densities remained constant throughout the testing procedure, this would also suggest that within one week of staling, the density is not yet affected by change in texture or structure.

The data provided by the Instron is likely less accurate than the calculations due to its load cell providing and recording stresses far beyond the requirements of tensile testing bread. Figure 31 below describes the daily averages of tensile stress compared to tensile strain of the best samples from the recorded Instron data.

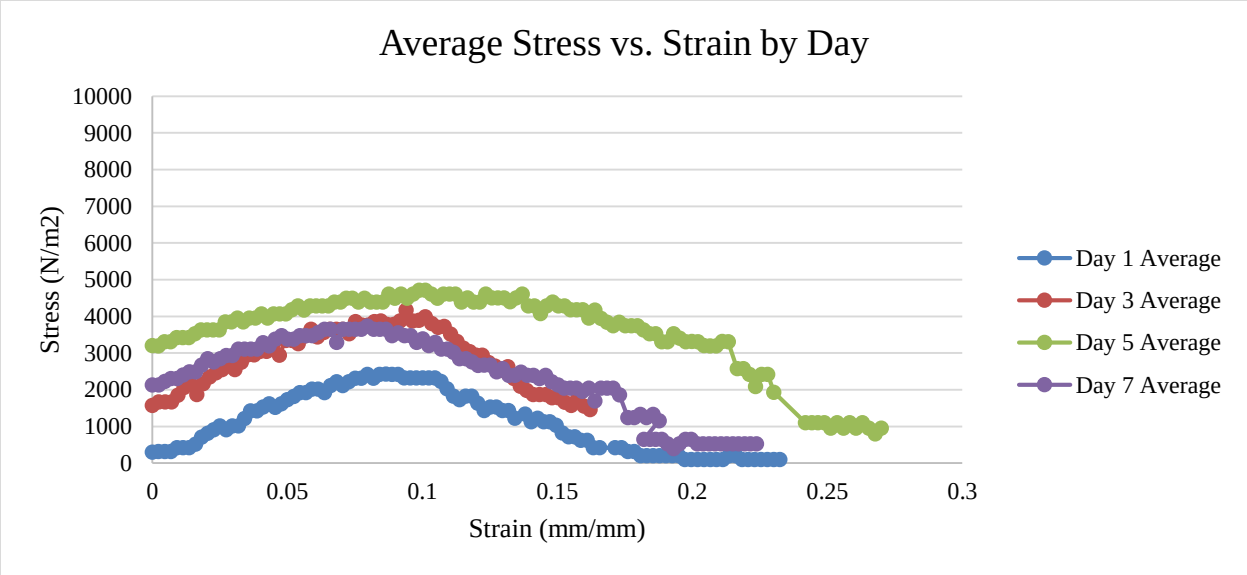

Figure 31: Average stress vs. strain by day for tensile samples.

The curves above follow a similar trend, and from these curves the experimental foam elastic modulus, yield strengths, and tensile strengths were recorded. These values, as shown in Table 6 below, are a result of graphical calculations, and are relatively similar – apart from the elastic modulus values.

Table 6: Sample strength and modulus values by day.

	Yield Strength (kPa)	**Ultimate Tensile Strength (kPa)**	**Modulus of Elasticity (kPa)**
DAY 1	2.429379	1.919863	35.17131
DAY 3	3.651364	4.171349	62.15023
DAY 5	3.954506	4.709341	125.8103
DAY 7	3.474562	3.735857	72.70044
AVG	3.377453	3.634102	73.95808

Although the concepts of growth rate and crack propagation under a cyclical stress are significant topics within general mechanical properties of tensile specimens, in the instance of bread, which is best described as an “elastic-brittle foam”, cyclical stresses are usually not applied due to crack propagation under an immediate load (Gibson & Ashby, 1999). In each instance of experimental data, there is only one cyclic load applied, eliminating the need to address multiple

cycles. As a result, the elongation prior to fracture is more relevant in the investigation of bread crumb and utilization of equations through the literature referenced in this report.

5.2.2 COMPARISON TO LITERATURE

As previously addressed, the constant C1 value was obtained through experimental calculation. The literature provides a constant k, which can also be used in calculations regarding the relative and solid elastic modulus from a given foam modulus. Table 7 below compares the resulting values from using the literature constant and the experimental constant.

Table 7: Comparison of constants, given versus experimental.

		Literature Constant k			**Calculated Constant C1**		
	E* (kPa)	E (kPa)	Es (kPa)	σ_{el} (kPa)	E (kPa)	Es (kPa)	σ_{el} (kPa)
DAY 1	35.17131	0.345763	101.7209	1.7585653	0.412548	85.25376	29.47757
DAY 3	62.15023	0.421259	147.5346	3.1075113	0.526845	117.9668	49.69453
DAY 5	125.8103	1.228028	102.4491	6.2905163	2.009221	62.61647	76.89479
DAY 7	72.70044	1.080754	66.03767	3.5685238	1.706644	41.8192	45.19627
AVG	73.95808	0.716062	102.8201	3.6812792	1.013059	72.67648	52.04087

The modulus values are relatively similar, with less consistency in the later days of trials, which is addressed in the next section of this chapter. The value of the force on the open cells, σ_{el}, was calculated using the following equation:

$$\frac{\sigma_{el}}{E_s} = 0.05 * \left(\frac{\rho^*}{\rho_s}\right)^2$$

As the solid elastic modulus is included in the calculation, the difference in values between the literature and the previously calculated constants became significant, with the resulting values found in Table 7 above. The values obtained using the literature have little variation, yet differ significantly from the values obtained using the experimentally calculated constant. In the graphs below, the open-cell force in the elastic region of the daily averages are displayed. It should be noted that, apart from Day 5, the open-cell force takes a shorter period of time to reach its maximum as the samples grew stale.

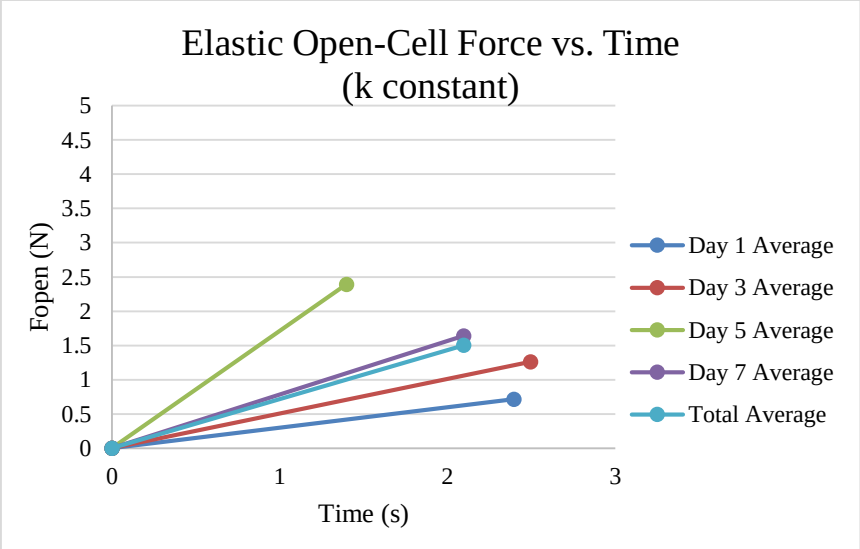

Figure 32: The elastic open-cell force vs. time, as calculated with the given constant k=1.

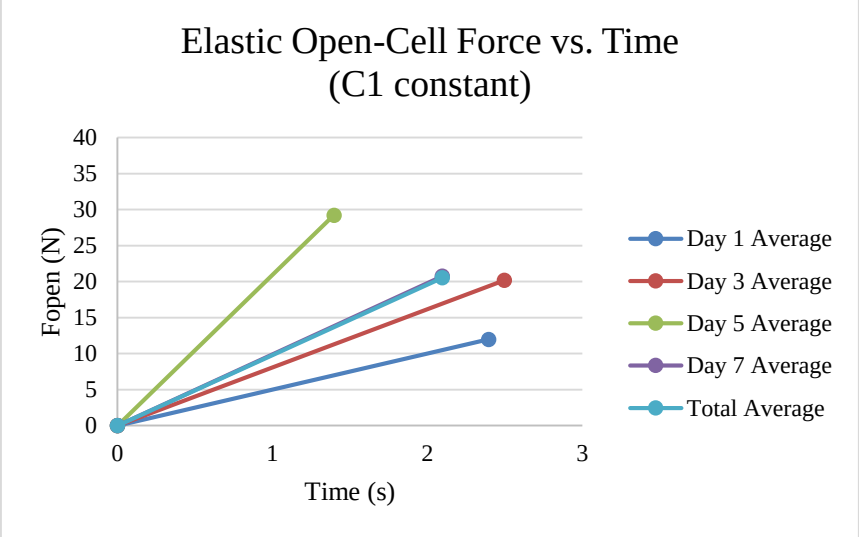

Figure 33: The elastic open-cell force vs. time, as calculated with the constant C1 by experimental value.

A noticeable trend in the recorded data and graphs in Figures 32 and 33 above includes the increased starting force in the recorded Instron data from the later days of testing. When observing data from Days 5 and Day 7 of testing, at a strain of 0 mm/mm, it is clear that the stress begins beyond a value of 0 N/m^2. This inconsistency, starting in the middle of Day 3 testing, can be attributed to either the staling of the bread or potentially handling the samples in such a way that the fracture of cell structures began prior to tensile testing. Beginning with a greater initial force

appears to eliminate the elastic region of testing, largely affecting the elastic modulus, which can be seen in the graph comparison in Figure 34 below.

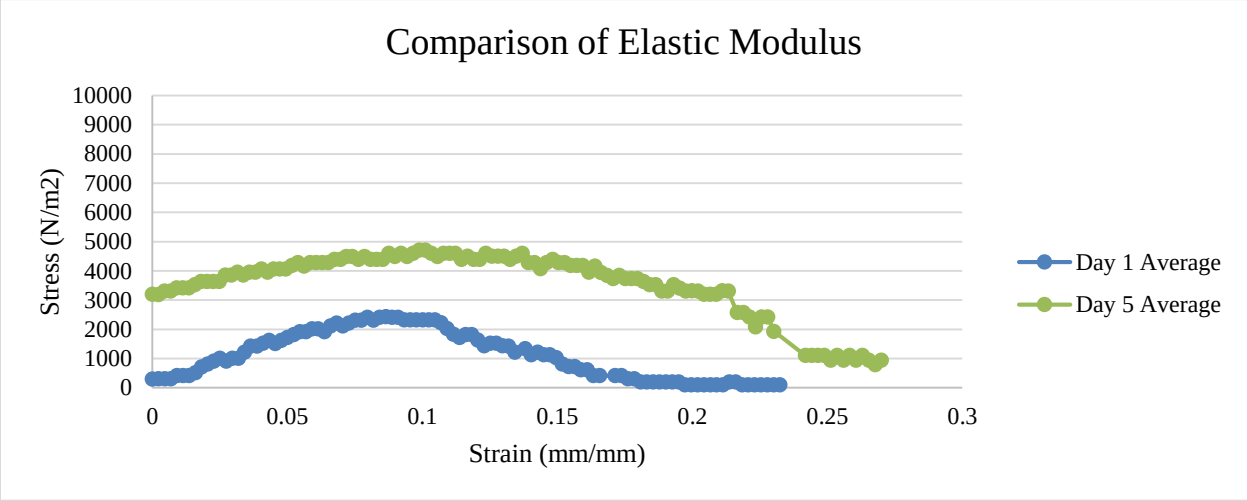

Figure 34: Comparison of the effect of elastic modulus during linear behavior.

As illustrated in the figure, it appears that the initial stress value has a significant impact on the stress values throughout the tensile test, and with this information it should be noted that Day 1 and Day 3 of testing yield the most consistent and accurate results.

5.3 Comparison of Graphical Plots

In order to create a cohesive report that illustrates the fracture pattern of bread crumb both visually and graphically, the results were compiled in such a way that one can visually observe the impact of the force applied and relate it to the graphical evidence presented by the Force vs. Time curves. Three samples, as illustrated below, were specifically chosen in order to provide visual evidence of fracture patterns during tensile testing.

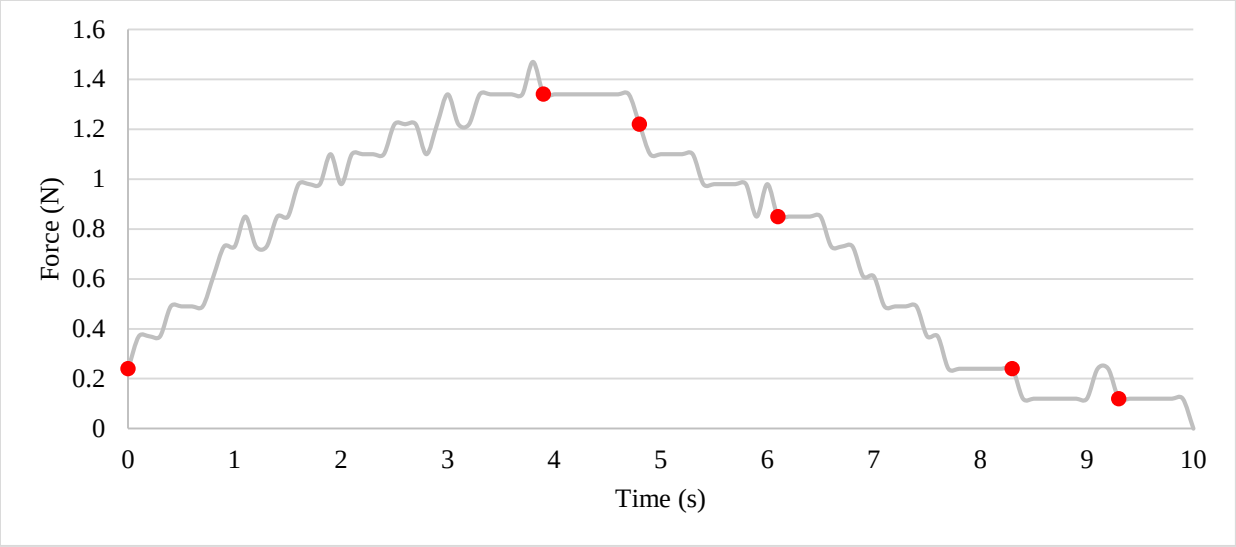

Figure 35: Day 1 Sample 10 Force vs. Time Graph

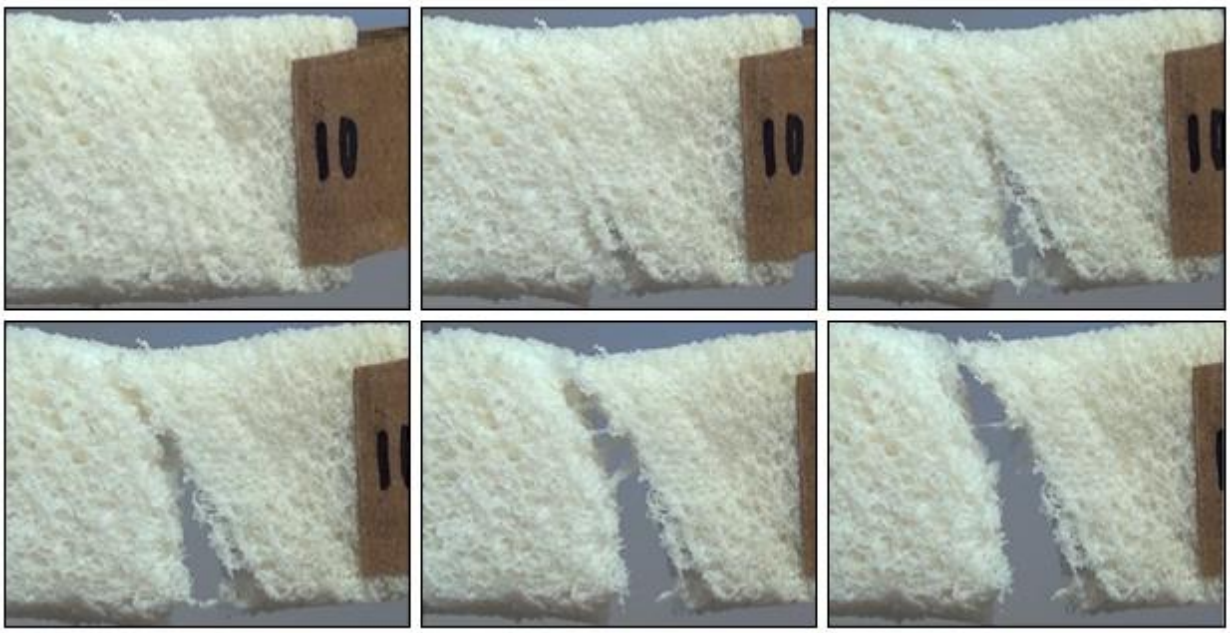

Figure 36: Time lapse of Day 1 Sample 10 photos during fracture.
Each photo associated with the marked points on the graph in Figure 35.

In the first chosen sample, respective to Figures 35 and 36 above, the tensile fracture occurred at an angle in the central area of the sample. The graphical plot shows the Force vs. Time curve of Sample 10, while the six consecutive images display the sample at specific points during the tensile test, represented by six red markers. The first image shows no noticeable areas where

one would assume the crack to propagate. Comparing the second and third photos, the edge of fracture follows a visually predictable path. The nature of fracture is illustrated in the twisting and snapping of the remaining cell wall structures as they diminish. After the maximum force is applied, the decline of the curve highlights the fracture of the cell walls in the final stages of the tensile test. At this level of magnification, cell structure beyond the cell is not significantly observed.

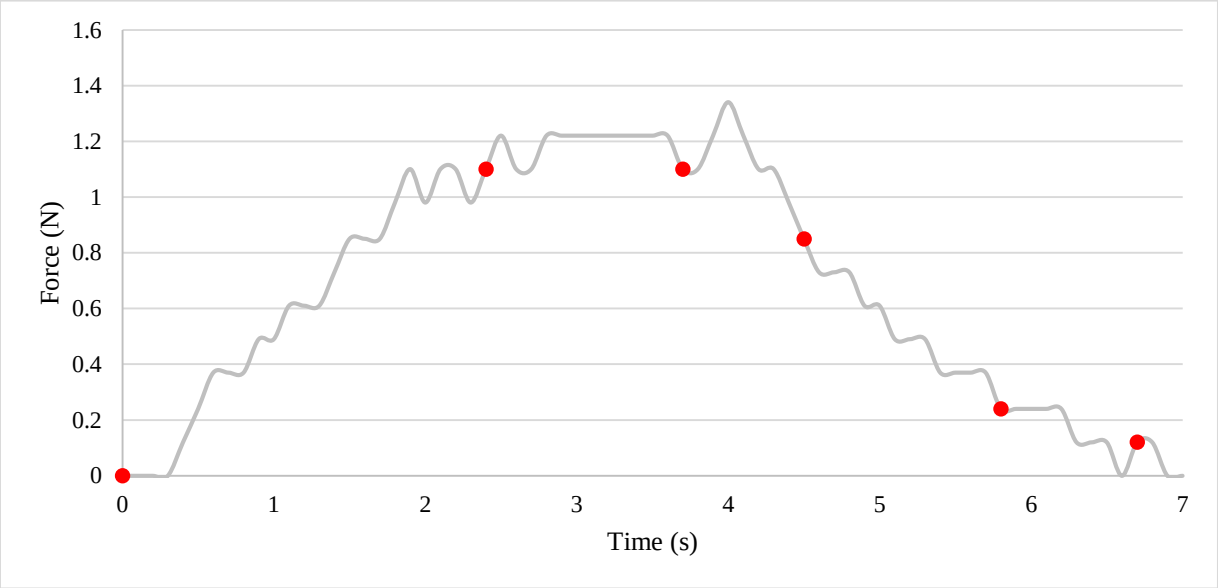

Figure 37: Day 3 Sample 7 Force vs. Time Graph

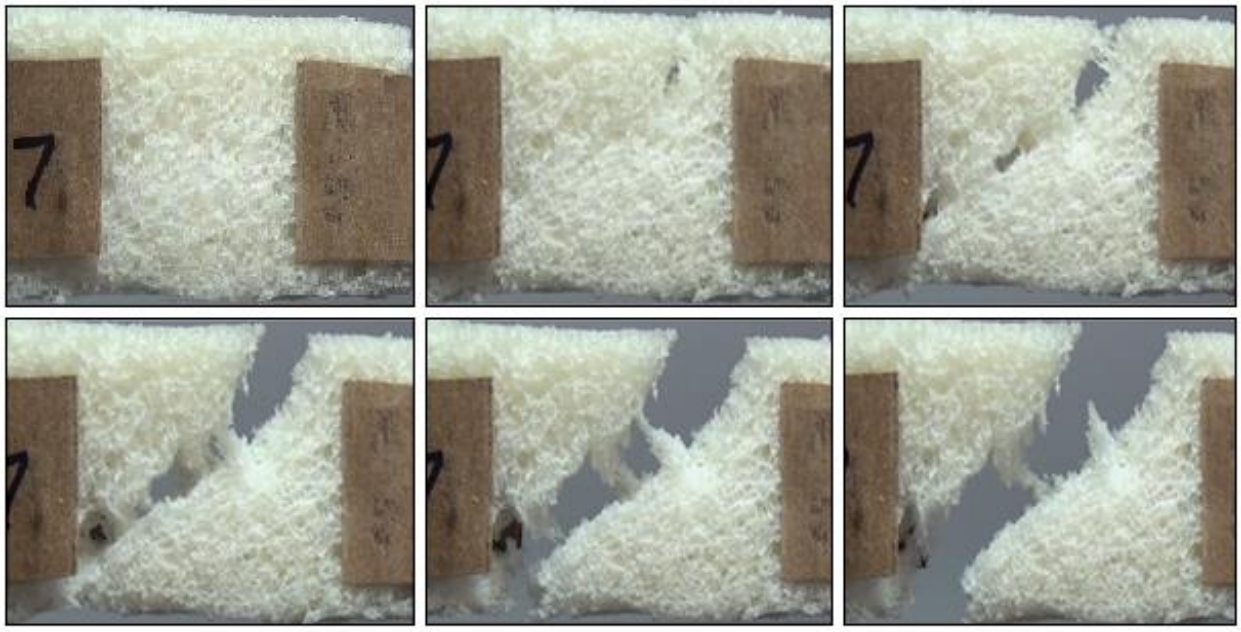

Figure 38: Time lapse of Day 3 Sample 7 photos during fracture.
Each photo associated with the marked points on the graph in Figure 37.

The second sample, presented in the graphical plot in Figure 37 and an additional six consecutive photographs in Figure 38 above, also fractured at an angle with the crack propagating slightly off from the center of the sample, but still breaking through the center. The same behavior is seen with the stronger cell walls remaining connected for a longer portion of the tensile test, with the applied force fluctuating closer towards the end of the test. When observing the images from Sample 7, the fracture path can also be seen, in that the cell walls along the fracture edge appear to be narrower than those of the rest of the sample, which may have been a cause for fracture at that particular location. This may be an indication of transcellular fracture, as the crack moves at an angle, likely breaking around cells which are aligned in a varying, non-linear fashion.

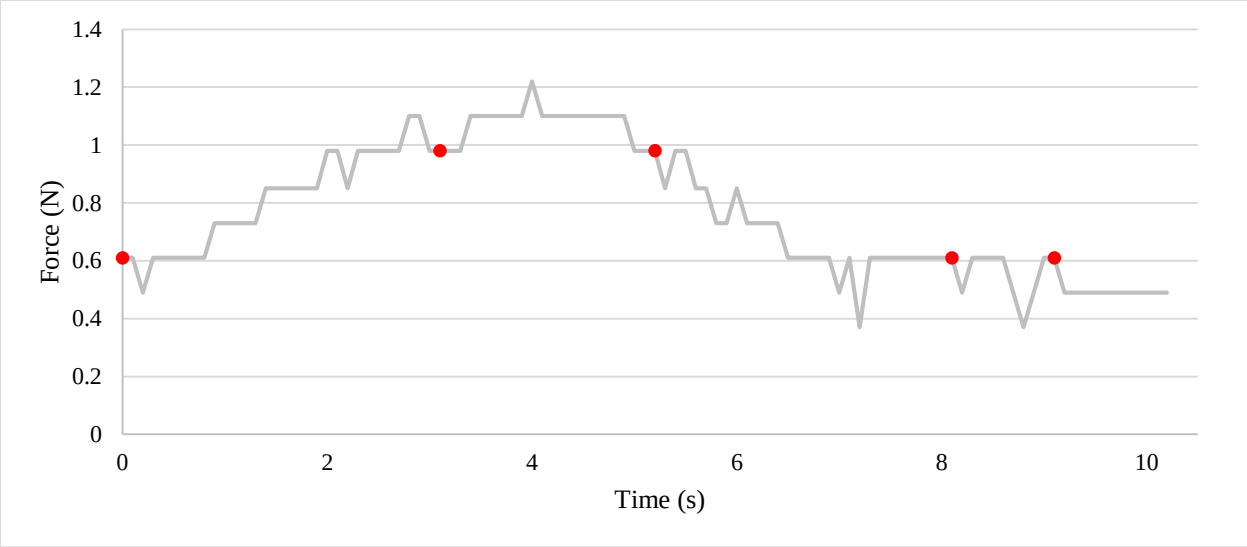

Figure 39: Day 7 Sample 11 Force vs. Time Graph

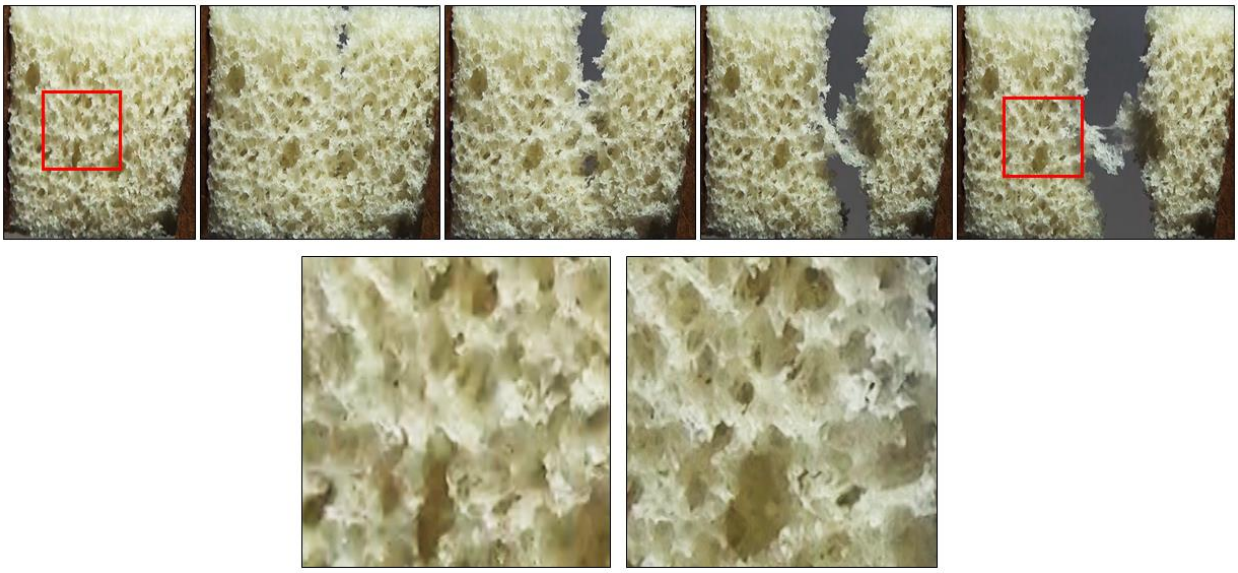

Figure 40: Time lapse of Day 7 Sample 11 photos during fracture. Each photo associated with the marked points on the graph in Figure 39. Additional magnification of 4x provides cell analysis in the bottom photos of the figure.

Figures 39 and 40 above display the third chosen sample at specific times throughout the tensile test and the corresponding photographs. The five consecutive photos show the gradual fracture path, which is located in the center of the bread sample. The two areas of the sample outlined in red are zoomed in 4x and displayed below the consecutive images for a closer look. The expanded photographs show the same exact area of the sample as the sectioned outlined in

red on the first photo before and the last photo after the tensile test in order to display the change in pore size of the bread. By examining the two pores located at the top center of each expanded image and the single pore located at the bottom center of each expanded image, it is clear that the three pores did not change in size vertically, but drastically changed in size horizontally. The tensile test performed on the sample applied a level of force that permanently stretched the bread sample, which resulted in a change in pore size.

By observation of the magnified images, the cellular shapes visible fall into the category of hexagonal prism and dodecahedral prism, as initially stated in the literature. This observation supports the decision made to perform calculations with a 50/50 ratio of hexagonal and dodecahedral prisms in the equations given. The change in cellular structure as a result of force can be seen in the figure. Under a given uni-axial force, the cellular structure expands in the direction of the load. When the cellular structure experiences its maximum stress, fracture occurs either intracellularly or transcellularly, likely related to the direction of the cellular structure in relation to the direction of the axial load.

In each instance, the fracture pattern is unique while the data remains roughly the same as the other samples. In regard to growth rate, the data in Table 8 below highlights pertinent values for calculation.

Table 8: Growth rate of presented samples.

Sample	Total Time (s)	Crack Propagation Time (s)	Width (cm)	Growth Rate (cm/s)
D1S10	9.9	4	3	0.508475
D3S7	7	3.4	3.4	0.944444
D7S11	10.2	4	3.6	0.580645

A notable difference in growth rates can be related to the nature of the crack propagation. Sample 7 from the third day of testing has a significantly higher growth rate, which can be

accounted for by the use of the sample width to calculate the rate of crack growth. In the sample fracture, the total distance of the crack is greater than that of the width of the sample, as it cracks in a notably diagonal manner.

5.4 Comparison of Microscopic Images

Microscopic images of the bread crumb were analyzed in order to determine fracture patterns and to notice any notable changes in cell structure. While the initial and post-fracture images do not illustrate the same exact location of the sample, they provide insight to the changes that occur in the general structure that makes up bread crumb, as displayed in Figure 41 below.

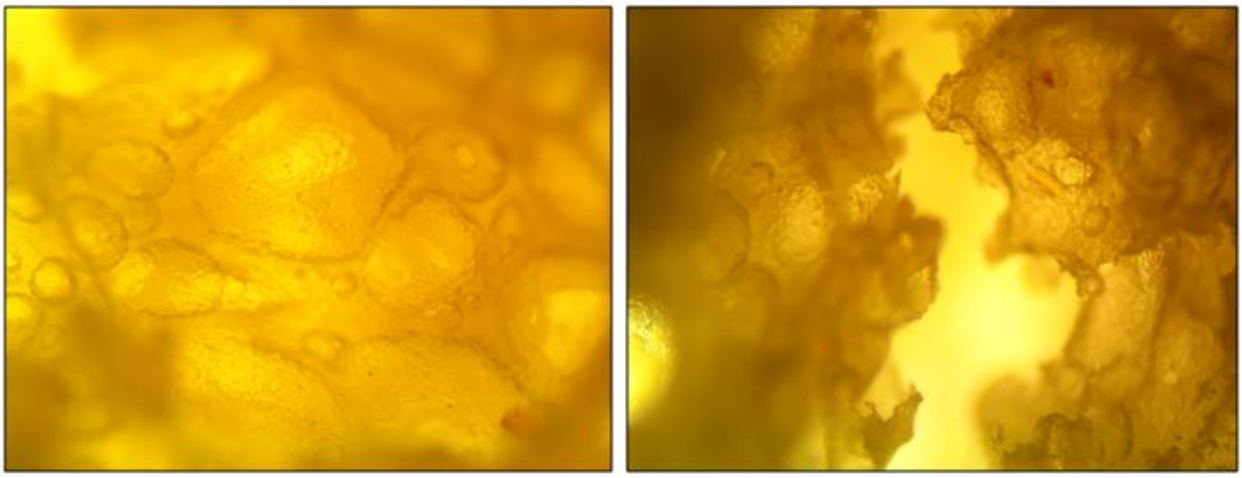

Figure 41: Pre- and post-fracture microscopic analysis of bread crumb.

The nature of cell wall fracture is illustrated in the post-fracture images. By observing the smaller, closed cells, it appears that the structure is retained, potentially as a result of the cell wall thickness surrounding the cells. Both intracellular and transcellular fracture can be found among the samples, as displayed in Figure 42 below. The images are of the same fracture, yet slightly shifted to provide perspective on the nature of the fracture.

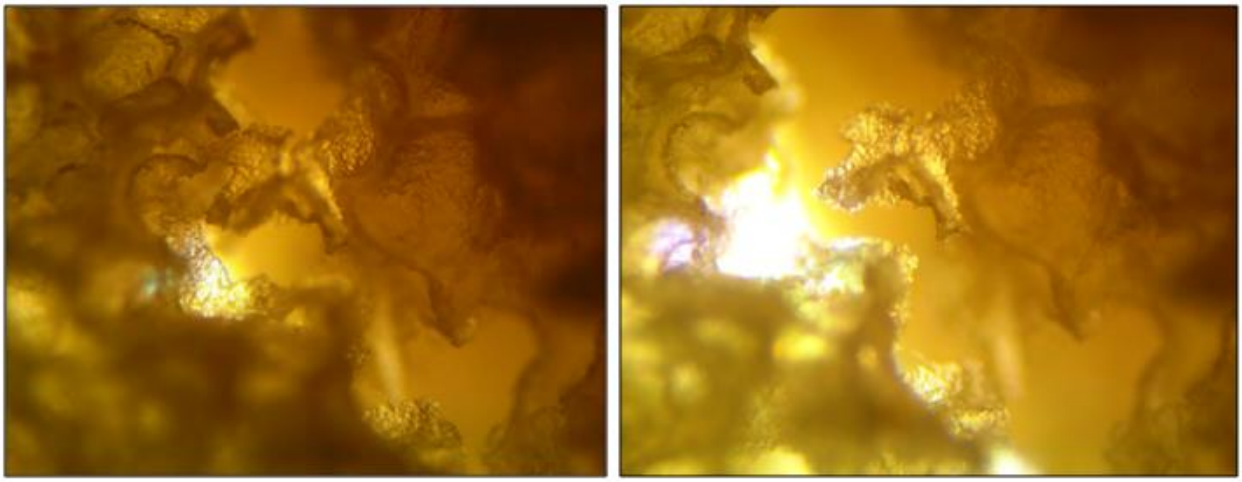

Figure 42: Post-fracture analysis of the break in cell wall structure.

Post-fracture analysis was also affected by the loss of crumb during tensile testing and sample handling. During microscopic analysis, crumb often broke off from the samples entirely. The variation in cellular structure between samples was evident in the examination process before and after fracture. Some samples had greater variance in the crumb structure, having little solid material lying the same vertical distance from the microscope. With the given magnification, difficulty capturing a clear image ensued.

In terms of the open and closed cells of the microscopic imagery, MagniSci software provided the results in the following Figure 43 through a two-dimensional analysis. On average, the ratio of open and closed cells was roughly 50/50, as evident in the images below. The accuracy of these findings would be enhanced with the use of an x-ray machine that is capable of three-dimensional measurement, yet it should be noted that with this method of data acquisition, the open-closed cell ratios were relatively precise, near the 50/50 mark.

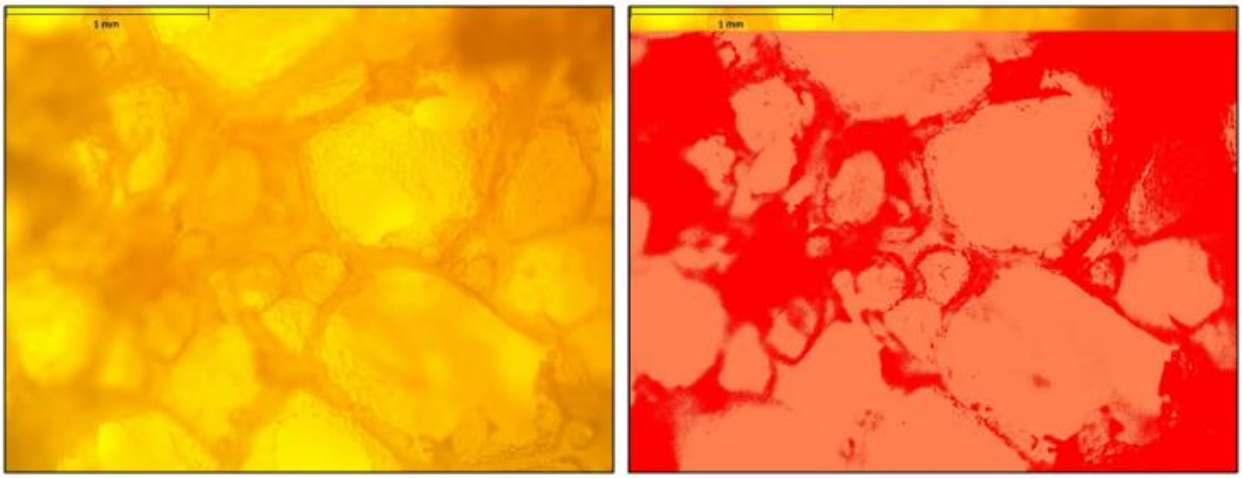

Figure 43: MagniSci analysis report of cell fraction, yielding a 50/50 ratio of open to closed cells.

The same sample is shown post-fracture below in Figure 44. Similar to the previously shown fracture samples, both intracellular and transcellular fracture can be seen. The focus of the post-fracture sample was more difficult to acquire as a potential result of the sample breaking in such a way that the sample became angled, having a change in cellular structure in the three planar dimensions.

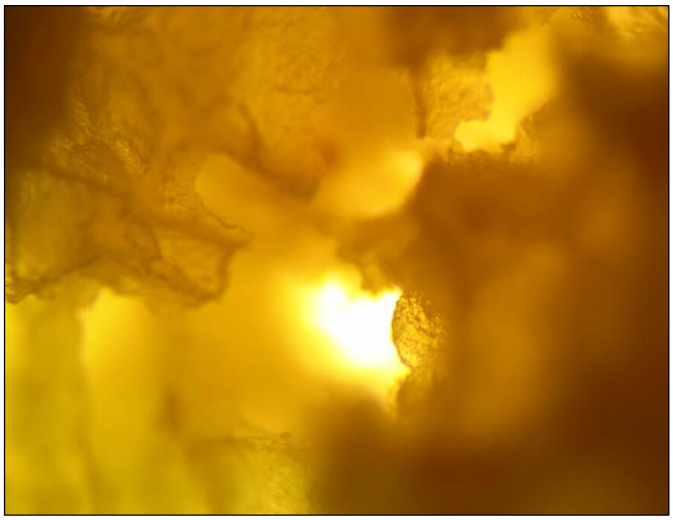

Figure 44: Fracture zone of bread crumb, note the angled break.

The fracture in most instances occurred at an angle through the center of the sample, with few samples breaking in a straight line down the center. In the microscopic image above, it is clear

that the fracture pattern is roughly a 45° angle along the center of the sample, which was found to be a common trend throughout tensile testing. This may be a result of the different cellular structures and orientations, yielding cell wall thicknesses experiencing stresses in different directions.

CHAPTER 6: CONCLUSIONS

A digital model for bread was developed to study the changes in cell structure when a compressive stress is applied. This model of the structure of bread was based on a combination of open and closed cells to best reflect the random nature of the foam structures in physical bread. Based on this digital model, rhombic dodecahedral cell shapes best represented the cellular structures created by MATLAB in order to illustrate open cells in a foam structure. Due to changes to the scope of this project, recommendations for future work include enhancing the digital model of bread crumb and 3D printing the respective model, which would incorporate another source, in addition to experimental data and published information, to improve the comparison of data.

Numerous trials in determining a standardized procedure were later executed in order to achieve the primary goal of examining the effect of stress on cell structure. This testing procedure allowed for the analysis of bread crumb and applicable calculations, as addressed throughout the report. This analysis of the effect of stress on cell structure concluded that the cellular shapes found were a combination of hexagonal prisms and rhombic dodecahedra, and the calculated constants associated with the different cellular structures were consistent with published results. Throughout the seven-day testing period, there were not any noticeable changes in staling data. Further recommendations for future work on this project include an extended testing period and the use of updated equipment, such as an Instron machine, to improve accuracy throughout tensile testing, and a digital recording device, to acquire enhanced footage and provide more insight to the sample fracture pattern as it occurs.

REFERENCES

ASM International. (2004). Introduction to Tensile Testing. Materials Park, Ohio, USA. Retrieved from www.asuminternational.org

Babin, P., Valle, G. D., Dendievel, R., Lassoued, N., & Salvo, L. (2005). Mechanical Properties of Bread Crumbs from Tomography Based Finite Element Simulations. *Journal of Materials Science*, 5867-5873.

Cauvain, S. P. (2007). *Technology of Breadmaking* (2nd ed.). Springer US.

Elmehdi, H. M., Page, J. H., & Scanlon, M. G. (2003). Using Ultrasound to Investigate the Cellular Structure of Bread Crumb. *Journal of Cereal Science*, 33-42.

Farahmand, B., & Nikbin, K. (2008). Predicting Fracture and Fatigue Crack Growth Properties. *Engineering Fracture Mechanics*, 2144–2155.

Gibson, L. J., & Ashby, M. F. (1999). *Cellular Solids.* Cambridge: Cambridge University Press.

Hug-Iten, S., Handschin, S., Conde, B., & Escher, F. (1999). Changes in Starch Microstructure on Baking and Staling of Wheat Bread. *Institute of Food Science, Swiss Federal Institute of Technology*, 255-260.

Liu, Z., & Scanlon, M. G. (2003). Modelling Indentation of Bread Crumb by Finite Element Analysis. *Biosystems Engineering*, 477-484.

Liu, Z., & Scanlon, M. G. (2003, September). Review Paper: Predicting Mechanical Properties of Bread Crumb. Winnipeg, Canada.

Moayedallaie, S., Mirzae, M., & Paterson, J. (2010). Bread Improvers: Comparison of a Range of Lipases with a Traditional Emulsifier. *Food Chemistry*, 495-499.

Mondal, A., & Datta, A. K. (2008). Bread Baking - A Review. *Journal of Food Engineering*, 465-474.

Scanlon, M. G., & Zghal, M. C. (2001). Bread Properties and Crumb Structure. *Food Research International*, 841-864.

Stampfli, L., & Nersten, B. (1995). Emulsifiers in Bread Making. *Food Chemistry*, 353-360.

The MathWorks, Inc. (2015). *Delaunay Triangulation*. Retrieved from MathWorks: http://www.mathworks.com/help/matlab/math/delaunay-triangulation.html

Valle, G. D., Chiron, H., Cicerelli, L., Kansou, K., Katina, K., Ndiaye, A., . . . Poutanen, K. (2014). Basic Knowledge for the Design of Bread Texture. *Trends in Food Science & Technology*, 5-14.

Wang, S., Austin, P., & Bell, S. (2011). It's A Maze: The Pore Structure of Bread Crumbs . *Journal of Cereal Science*, 203-210.

Wang, S., Karrech, A., Regenauer-Lieb, K., & Chakrabati-Bell, S. (2013). Digital Bread Crumb: Creation and Application. *Journal of Food Engineering*, 852-861.

Zghal, M. C., Scanlon, M. G., & Sapirstein, H. D. (2002). Cellular Structure of Bread Crumb and its Influence on Mechanical Properties. *Journal of Cereal Science*, 167-176.

Zhang, J., & Datta, A. K. (2006). Mathematical Modeling of Bread Baking Process. *Journal of Food Engineering*, 78-89.

APPENDIX A: DAY 1 MAGNISCI DATA

Table 9: Complete MagniSci data for the three best samples on Day 1.

	OVERALL %		OPEN CELL DIAMETER (µm)			CLOSED CELL THICKNESS (µm)		
SAMPLE #	Open Cells	Closed Cells	Average Horizontal	Average Vertical	Combined Average	Average Horizontal	Average Vertical	Combined Average
D1S3.2	53.96	46.04	34.721	34.915	34.818	25.68	28.686	27.183
D1S3.3	55.56	44.44	58.115	56.283	57.199	23.868	27.824	26.846
D1S3.4	63.52	36.48	106.77	100.596	103.683	30.493	34.15	32.321
D1S4.1	58.56	41.44	58.205	56.094	57.149	28.86	30.54	29.7
D1S4.2	32.01	67.99	46.998	46.926	46.962	36.746	27.13	31.938
D1S4.3	43.17	56.83	57.648	54	55.824	49.842	52.49	51.166
D1S4.4	46.5	53.5	74.155	73.21	73.682	40.246	40.512	40.379
D1S10.1	64.92	35.08	96.32	94.056	95.188	41.691	35.379	38.535
D1S10.2	59.68	40.32	108.299	109.728	109.013	41.397	32.18	36.788
D1S10.3	56.89	43.11	83.113	78.344	80.729	45.092	43.301	44.196
D1S10.4	56.57	43.43	116.518	103.903	110.21	36.04	41.719	38.88
D1S10.5	49.87	50.13	75.795	72.305	74.05	43.362	64.275	53.819
AVG	53.43	46.57	76.39	73.36	74.88	36.94	38.18	37.65

APPENDIX B: DAY 3 MAGNISCI DATA

Table 10: Complete MagniSci data for the three best samples on Day 3.

	OVERALL %		OPEN CELL DIAMETER (µm)			CLOSED CELL THICKNESS (µm)		
SAMPLE #	Open Cells	Closed Cells	Average Horizontal	Average Vertical	Combined Average	Average Horizontal	Average Vertical	Combined Average
D3S5.1	68.58	31.42	82.628	77.557	80.093	35.958	37.789	36.874
D3S5.2	56.74	43.26	68.965	67.085	68.025	49.499	44.42	46.96
D3S5.3	60.35	39.65	73.488	71.017	72.252	37.375	38.659	38.017
D3S5.4	55.16	44.84	74.51	71.637	73.073	49.444	49.785	49.615
D3S7.1	61.26	37.74	75.493	71.069	73.281	39.832	36.413	38.122
D3S7.2	71.77	28.23	89.637	89.876	89.757	35.623	34.363	34.993
D3S7.3	58.97	41.03	82.916	82.332	82.624	43.217	39.57	41.393
D3S7.4	70.2	29.8	82.544	82.66	82.602	33.551	27.842	30.696
D3S10.1	60.25	39.75	54.241	52.572	53.406	29.139	29.607	29.373
D3S10.2	65.52	34.48	71.009	70.396	70.703	60.366	31.361	30.864
D3S10.3	56.26	43.74	75.229	72.334	73.816	43.176	48.597	45.886
D3S10.4	60.88	39.12	76.618	79.335	77.976	49.088	47.022	48.055
AVG	62.16	37.76	75.61	73.99	74.80	42.19	38.79	39.24

APPENDIX C: DAY 5 MAGNISCI DATA

Table 11: Complete MagniSci data for the three best samples on Day 5.

	OVERALL %		OPEN CELL DIAMETER (µm)			CLOSED CELL THICKNESS (µm)		
SAMPLE #	Open Cells	Closed Cells	Average Horizontal	Average Vertical	Combined Average	Average Horizontal	Average Vertical	Combined Average
D5S4.1	60.17	39.83	128.231	127.415	127.823	65.256	56.909	61.082
D5S4.2	54.23	45.77	72.309	69.862	71.086	42.603	36.777	39.69
D5S4.3	52.84	47.16	53.259	50.518	51.889	41.784	39.586	40.685
D5S4.4	39.27	60.73	43.484	44.167	43.826	38.208	38.628	38.418
D5S4.5	62.8	37.2	85.542	82.709	84.125	34.607	34.447	34.527
D5S5.1	55.87	44.13	108.806	103.062	105.934	68.431	61.046	64.738
D5S5.2	28.41	71.59	70.68	68.097	69.388	94.518	110.816	102.667
D5S5.3	37.9	62.1	84.357	81.226	82.791	74.358	54.217	64.287
D5S5.4	55.37	44.63	54.993	52.495	53.744	44.83	52.017	48.424
D5S5.5	59.59	40.41	116.386	117.838	117.112	53.426	47.047	50.25
D5S10.1	43.33	56.67	128.325	118.654	123.489	77.796	59.618	68.707
D5S10.2	44.01	55.99	59.292	54.619	56.955	56.444	47.73	52.087
D5S10.3	41.03	58.97	57.401	55.762	56.582	57.321	58.968	58.144
D5S10.4	43.92	56.08	59.392	58.45	58.921	65.59	57.241	61.416
D5S10.5	54.94	45.06	102.334	102.083	102.208	45.094	43.778	44.436
AVG	48.91	51.09	81.65	79.13	80.39	57.35	53.26	55.30

APPENDIX D: DAY 7 MAGNISCI DATA

Table 12: Complete MagniSci data for the three best samples on Day 7.

	OVERALL %		OPEN CELL DIAMETER (µm)			CLOSED CELL THICKNESS (µm)		
SAMPLE #	Open Cells	Closed Cells	Average Horizontal	Average Vertical	Combined Average	Average Horizontal	Average Vertical	Combined Average
D7S3.1	49.77	50.23	65.231	68.482	66.857	38.514	36.736	37.625
D7S3.2	40.73	59.27	56.876	55.357	56.117	56.51	55.727	56.118
D7S3.3	36.99	63.01	44.617	44.871	44.744	46.037	44.357	45.197
D7S3.4	46.62	53.38	50.584	49.62	50.102	52.893	48.182	50.537
D7S3.5	49.68	50.32	62.457	65.034	63.745	54.864	60.206	57.535
D7S6.1	48.7	51.3	95.989	92.226	94.108	51.324	53.851	52.588
D7S6.2	47.16	52.84	76.823	74.85	75.836	54.704	52.854	53.779
D7S6.3	43.62	56.38	53.393	52.244	52.818	53.784	46.781	50.282
D7S6.4	42.77	57.23	74.272	72.607	73.439	33.562	33.43	33.496
D7S6.5	44.26	55.74	68.646	70.446	69.546	54.27	54.872	54.571
D7S11.1	51.9	48.1	134.889	131.614	133.251	80.883	77.03	78.957
D7S11.2	44.95	55.05	92.039	93.51	92.775	53.674	44.081	48.877
D7S11.3	57.5	42.5	150.143	149.042	149.592	70.491	43.776	57.133
D7S11.4	49.09	50.91	77.629	81.641	79.635	47.564	46.054	46.809
D7S11.5	50.25	49.75	59.264	58.477	58.871	40.402	43.685	42.043
AVG	46.93	53.07	77.52	77.33	77.43	52.63	49.44	51.04

APPENDIX E: MATLAB CODE: BREADGEN

```
%% Initialization, clears all existing variables and stored information.
clc; clear all; close all;

%% Stating the required information to be provided in order to form a cellular figure.
% Shapes = [r1 n1 x1 y1 z1;
%         r2 n2 x2 y2 z2;
%         . . . . . ;
%         . . . . . ;
%         . . . . . ;
%         rN nN xN yN zN];

%% Setting the outer dimensions of the slice of bread.
a = 1.5;
b = 5;
c = 7.5;
X = [a/2;b/2;c/2];

%% Allows the outer slice dimensions to be plotted on the same graph as the cellular figures, sets
the axis.
FH = figure();
hold on;
axis([-0.1 a -0.1 b -0.1 c]);

%% Bread Outline – Calls to the function 'box2data' to provide the right format of data for plotting
the outer slice of bread.
BOP = box2data([a b c X']);

%% Cellular Figures – Sets the maximum and minimum diameter for the cellular figures, provides
the maximum volume allowed and the initial number of cellular figures to be created.
LL = 0.08;  % Low Limits
HL = 0.1;   % High Limits
v_desired = 3/4*HL^3;
N = 500;    % Number

%% Randomly assigns cellular dimensions and locations remaining within the limitations of the
figure and stores them in a list.
r = interp1([0 1],[LL HL],rand(N,1));
u = 6*ones(N,1);
x = interp1([0 1],[HL a-HL],rand(N,1));
y = interp1([0 1],[HL b-HL],rand(N,1));
z = interp1([0 1],[HL c-HL],rand(N,1));
HexList = [r u x y z];
```

```
%% The function 'hex2data' is utilized to acquire the data from the created list in a different format so that the cells can be plotted.
for n=1:N
  P(:,:,n) = hex2data(HexList(n,:));
end

%% Utilizes the 'box2data' function to format the data in the list so that it can be plotted.
M = box2data(BOP);

%% Finding colliding boxes and combining them – Starting with an empty list, the function 'collisionDetection_II' utilized to check for cellular figures that have the same located dimensions.
[List] = collisionDetection_II(HexList);
cN = size(List,1);
Total_volume = 0;

%% Looking through the entire list of cellular figures, this adds to the new list 'List' to add the data for points that collide.
for n=1:cN
   TM = [];
   cList = List{n};
   for m=cList
      pN = size(P(:,:,m),1);
      TM(end+1:end+pN,:) = P(:,:,m);
   end

%% Reviews the new list 'List' to determine if new volumes exceed the maximum volume, and if so creates a message stating so and establishing a new volume for the cellular figure by eliminating one of the colliding figures.
   [Mtemp,v,TR] = points2mesh(TM,-1);
   if(v > v_desired)
      fprintf('-- The volume of %.6f is greater than %.6f\n',v,v_desired);
      x_center = mean(TM(:,1));
      y_center = mean(TM(:,2));
      z_center = mean(TM(:,3));
      r = interp1([0 1],[LL HL],rand());
      TM =  hex2data([r 6 x_center y_center z_center]);
      [Mtemp,v,TR] = points2mesh(TM,-1);
      fprintf('=> New volume = %.6f\n',v);
   end

%% Gathers the total volume of the cellular figures that exist in the slice of bread and creates a matrix of the points.
   Total_volume = Total_volume + v;
   Mtemp_R = size(Mtemp,1);
   M(end+1:end+Mtemp_R,:) = Mtemp;
end
```

```
%% Get rid of the colliding boxes.

%% Makes a one-column matrix of all the rows in the matrix containing all the rectangles that collide.
G = []; %start with empty matrix
for n=1:length(List)
   innerList = List{n};
   for m=1:length(innerList)
      G(end+1,1) = innerList(m);
   end
end

%% Gathers data from the list 'List' to enter into this matrix.
P(:,:,G) = [];
N = size(P,3);
HexList(G,:) = [];

%% Mesh the remaining boxes so they can be plotted.
for n=1:N
  [newMesh, v] =  hex2data(P(:,:,n));
  row =  size(newMesh,1);
  M(end+1:end+row,:) = newMesh;
  Total_volume = Total_volume + v;
end

%% Plot the final results on the same figure.
plotMesh(M,'c',0.2, FH);

%% Convert to STL so that a solid part can be opened in SolidWorks.
convert2stl(M,'Test');
```

APPENDIX F: MATLAB CODE: COLLISIONDETECTION_II

```
%% Provides the input and output required for the function to work properly.
function [List] = collisionDetection_II(hexList)

%% Establishes an initially empty list.
N = size(hexList,1);
CollisionList = [];

%% If the distance between two cellular figure centers is less than the sum of their radiuses, the
points are added to the collision list.
for n=1:N
   for m=n+1:N
      R1 = norm(hexList(n,3:5)' - hexList(m,3:5)');
      R2 = hexList(n,1)+hexList(m,1);
      if ( R2 >= R1 )
         CollisionList(end+1,:) = [n,m];
      end
   end
end

%% Calls to the function 'CloseCollision' to specify exactly which cells collide with each other to
create a proper list.
List = CloseCollision(CollisionList);
```

APPENDIX G: MATLAB CODE: CLOSECOLLISION

%% Compares the list including more than enough information associated with the colliding parts and picks out the necessary information to combine the cellular figures into one.

```
function [List] = CloseCollision(C)

%% Goes through the list and finds the correct cellular figure information to pair the colliding parts.
if(isempty(C))
   List = [];
else
   j = 1;
   while (~isempty(C))
      g = C(1,1);
      k = 1;
      while(1)
         if(k > length(g))
            break
         end
         s = g(k);
         sc1 = find(C(:,1)==s);
         sc2 = find(C(:,2)==s);
         for n=sc1'
            g(end+1) = C(n,2);
         end
         for n=sc2'
            g(end+1) = C(n,1);
         end
         C([sc1',sc2'],:) = [];
         k = k + 1;
      end
      List{j,1} = g;
      j = j + 1;
   end
end
```

APPENDIX H: MATLAB CODE: BOX2DATA

```
%% Turns the information stored for a rectangular figure into data that can be meshed and plotted.
function [data] = box2data(box)

%% Establishes box information and finds the correct location in the matrix for each variable.
[M,N] = size(box);
if(M==1) % If the input represents a box information as l w t x y z
   l = box(1);
   w = box(2);
   t = box(3);
   x = box(4:6);

%% Finds the centers of the variables.
   l_ = l/2;
   w_ = w/2;
   t_ = t/2;

%% Creates and stores the normal faces of each triangular face on the rectangular prism.
   data(1,:) = [-l_ , -w_ , -t_] + x;
   data(2,:) = [l_ , -w_ , -t_] + x;
   data(3,:) = [l_ , w_ , -t_] + x;
   data(4,:) = [-l_ , w_ , -t_] + x;
   data(5,:) = [-l_ , -w_ , t_] + x;
   data(6,:) = [l_ , -w_ , t_] + x;
   data(7,:) = [l_ , w_ , t_] + x;
   data(8,:) = [-l_ , w_ , t_] + x;

%% Turns the data into a mesh, as all required information is available to do so.
else % if input is the points defining a box => convert it to a mesh
   data = [box(1,:) box(2,:) box(6,:) 0 -1 0;
         box(1,:) box(5,:) box(6,:) 0 -1 0;
         box(2,:) box(3,:) box(4,:) 0 0 -1;
         box(2,:) box(1,:) box(4,:) 0 0 -1;
         box(2,:) box(3,:) box(7,:) 1 0 0;
         box(2,:) box(6,:) box(7,:) 1 0 0;
         box(6,:) box(7,:) box(8,:) 0 0 1;
         box(6,:) box(5,:) box(8,:) 0 0 1;
         box(3,:) box(4,:) box(8,:) 0 1 0;
         box(3,:) box(7,:) box(8,:) 0 1 0;
         box(1,:) box(4,:) box(8,:) -1 0 0;
         box(1,:) box(5,:) box(8,:) -1 0 0];
end
```

APPENDIX I: MATLAB CODE: HEX2DATA

```
%% Turns the information on hexagonal prisms into data that can be turned into a mesh.
function [data,v] = hex2data(hex)

%% Establishes the hexagonal information in the matrix.
[M,~] = size(hex);
if(M==1) % If the input represents a hexagon information as r a h x y z
    r = hex(1);
    n = hex(2);
    X = hex(3:5);
    phi = linspace(-pi/2,pi/2,n/2+1);
    theta = linspace(0,2*pi,n+1);

%% Establishes location of the center by use of trigonometric equations.
    x = [];
    y = [];
    z = [];
    for i=1:length(phi)
        for j=1:length(theta)
            x(end+1) = r*cos(phi(i))*cos(theta(j));
            y(end+1) = r*cos(phi(i))*sin(theta(j));
            z(end+1) = r*sin(phi(i));
        end
    end

%% Provides inputs required to create the hexagonal prism and utilizes 'points2mesh' to create a
mesh.
    data = [x'+X(1) y'+X(2) z'+X(3)];
    v = NaN;
else
    [data,v,~]  = points2mesh(hex,-1);
end
```

APPENDIX J: MATLAB CODE: POINTS2MESH

```
%% Turns given data points into a mesh with the established inputs and outputs.
function [mesh,v,TR]  = points2mesh(X,direction)
% If the "direction" input is not available, Assume direction is 1
if(nargin == 1)
   direction = 1;
end

%% A Delaunay triangulation for a set P of points in a plane is a triangulation DT(P) such that no point in P is inside the circumcircle of any triangle in DT(P).
DT = delaunayTriangulation(X);

%% Find the points that form the boundary of the object where v is the volume of the bounded object.
[K, v] = convexHull(DT);
TR = triangulation(K,DT.Points);

%% Change the direction of the normal faces based on the input provided.
fn = direction*faceNormal(TR);

%% Convert them into a mesh.
for i=1:size(K,1)
   mesh(i,:) = [DT.Points(K(i,1),:) DT.Points(K(i,2),:) DT.Points(K(i,3),:) fn(i,:)];
end
```

APPENDIX K: MATLAB CODE: PLOTMESH

```
%% Already existing MATLAB function, plots any given meshed data.
function [FH] = plotMesh(M,Color,FaceAlpha,FigureHandle)

%% Checking for the inputs. If user has not provided face color and alpha (transparency), they are
assigned to be blue and 0.5.
if(~exist('Color','var'))
   Color = 'b';
end
if(~exist('FaceAlpha','var'))
   FaceAlpha = 1;
end
if(~exist('FigureHandle','var'))
   FH = figure();
else
   figure(FigureHandle);
end

%% Defining the number of triangles available in M.
N = size(M,1);

%% Initializing the plot by holding onto the previous figure and scaling/labeling the axes.
hold on;
axis equal
xlabel('x'); ylabel('y'); zlabel('z');

%% Adding transparent color to each figure and showing a 3D view.
for n=1:N
   fill3(M(n,[1 4 7]),M(n,[2 5 8]),M(n,[3 6 9]),Color);
end
alpha(FaceAlpha);
view(3)
```

APPENDIX L: MATLAB CODE: CONVERT2STL

```
%% Turns the MATLAB file into an STL file which can be opened as a solid part in SolidWorks.
function convert2stl(M,filename)

%% Returns a message with the file name.
N = size(M,1);
str = sprintf('solid %s\n',filename);
S = '   ';

%% Takes data from the solid body and creates the text format readable by an STL file.
for n=1:N
   face_normal = sprintf('%sfacet normal %E %E %E',S,M(n,10:12));
   loop = sprintf('%s%souter loop',S,S);
   vertex1 = sprintf('%s%s%svertex %E %E %E',S,S,S,M(n,1:3));
   vertex2 = sprintf('%s%s%svertex %E %E %E',S,S,S,M(n,4:6));
   vertex3 = sprintf('%s%s%svertex %E %E %E',S,S,S,M(n,7:9));
   eloop = sprintf('%s%sendloop',S,S);
   eface = sprintf('%sendfacet',S);
   str                                                                                    =
sprintf('%s%s\n%s\n%s\n%s\n%s\n%s\n%s\n',str,face_normal,loop,vertex1,vertex2,vertex3,eloo
p,eface);
end
str = sprintf('%sendsolid',str);

%% Finalizes the file and saves it in the same MATLAB folder.
fileID = fopen([filename,'.stl'],'wt');
fwrite(fileID, str);
fclose(fileID);
```